Spring 2016

Anthropometric human modeling on the shape manifold

Samuel Spicer Mate
University of Iowa

Anthropometric Human Modeling on the Shape Manifold

by

Samuel S. Mate

A thesis submitted in partial fulfillment
of the requirements for the Master of Science
degree in Mechanical Engineering
in the Graduate College of
The University of Iowa

May 2016

Thesis Supervisor: Assistant Professor Stephen Baek

Graduate College
The University of Iowa
Iowa City, Iowa

CERTIFICATE OF APPROVAL

_____

MASTER'S THESIS

_____

This is to certify that the Master's thesis of

Samuel S. Mate

has been approved by the Examining Committee for
the thesis requirement for the Master of Science degree
in Mechanical Engineering at the May 2016 graduation.

Thesis Committee: _____
Stephen Baek, Thesis Supervisor

_____
Hiroyuki Sugiyama

_____
Jia Lu

ACKNOWLEDGEMENTS

The author would like to acknowledge the members of the SantosHuman and Virtual Soldier Research groups for providing their insight and data that aided and enabled a good portion of this research. Additionally, Dr. Baek for lending his invaluable expertise in the field and providing the digital human model databases essential to this project. This research was additionally aided by the efforts of my co-workers in the IDEA Lab, namely the template model fitting work done by Zhiyu Sun.

ABSTRACT

The accuracy of modern digital human models has led to the development of human simulation engines capable of performing a complex analysis of the biometrics and kinematics / dynamics of a digital model. While the capabilities of these simulations have seen much progress in recent years, they are hindered by a fundamental limitation regarding the diversity of the models compatible with the simulation engine, which in turn results in a reduction in the scope of the applications available to the simulation. Additionally, a significant amount of time and expertise is required to make a digital human model compatible with the simulation. In this research I present a solution to this limitation by outlining a process to develop a set of mutually compatible human models that spans the range of feasible body shapes and allows for a "free" exploration of body shape within the shape manifold. Additionally, a method is presented to represent the human body shapes with a reduction of dimensionality, via a spectral shape descriptor, that enables a statistical analysis that is both more computationally efficient and anthropometrically accurate than traditional methods. This statistical analysis is then used to develop a set of representative models that succinctly represent the full scope of human body shapes across the population, with applications reaching beyond the research-oriented simulations into commercial human-centered product design and digital modeling. Additionally, these statistical clusters used to generate the representative models are used to redefine the anthropometric guidelines for clustering the population in a manner that offers significant benefits to areas such as garment design and human factors analysis.

PUBLIC ABSTRACT

The capabilities of digital human models has increased dramatically over the past few years, and as a result have played an increasing role in the design process. By utilizing a digital human model in the design process one can validate the use of the design without the need for prototyping, and as a result generate a significant amount of savings in the design stage. Beyond the commercial sector, many research groups have developed advanced human simulation software that are capable of performing an in-depth analysis of a human in a variety of situations, based off of the response of their digital human model. However, due to the complexity of the analysis it can be difficult to implement new human models into these software as there is a lack of compatibility between models. In both of these applications, the accuracy of the model used is imperative to obtain reasonable results.

This research presents a method capable of generating a set of digital human models that are all mutually compatible, thus allowing a more seamless implementation into a digital simulation software. Additionally, a process is outlined that can generate a representative set of human models from a statistical population analysis that is both more computationally efficient and anthropometrically accurate than traditional methods. These representative models then encompass the entire scope of human body shapes and can be used to validate designs across all demographics without the need for prototyping.

Additionally, the statistical clusters used to generate the representative models can be used to improve the anthropometric modeling of the human population. This, in turn, provides benefits to commercial sectors such as garment design as well as improving the capabilities of human factors analysis and human centered design.

Table of Contents:

List of Tables:

Table of Figures:

Chapter 1: Introduction:

1.1 - Background

Before discussing the background of the modeling methods specific to the research in this paper it is prudent to provide a brief history of the progression of the modeling methods so as to establish the terminology essential to the comparison of the results. The first step towards this end is to outline the various methods currently available for human body shape modeling. These methods can be efficiently categorized into four categories, including: (1) Direct model acquisition / creation, (2) Template model-based scaling, (3) Image-based reconstruction, and (4) Statistics-based model synthesis [Baek2012].

The direct model creation methods refer to processes such as 3D scanning of the human form and anatomical model construction. As it currently stands, the 3D scanning method of model acquisition is certainly the most accurate method and has seen a growth of popularity with the increased capabilities of 3D scanning technology, although the high equipment costs still remain as a lingering deterrent. Anatomic reconstruction methods also result in accurate models, however, due to their fabrication from the derivation of a "skin" over a system of the underlying internal structures. By initially modeling the muscles, bones, etc. the resultant body shapes are quite plausible. However, these methods are poorly compatible with most CAD systems as they require a vast knowledge base of the internal structure of the human body which is often not of any import in the use of a digital human model. The additional effort of modeling the interior structures then results in significant additional modeling costs with no added benefit to most applications.

Template model-based scaling methods refer to the process of synthesizing a new model via the deformation of a single template human body model. Once a template model has been prepared, its segments and proportions can then be scaled and adjusted to create additional body shapes. The simplicity, and resultant affordability, offered by this method has led to many applications within commercialized systems. This method, however, has an inherent lack of reliability in that there is no intrinsic correlation between the body parts and as such is subject to a loss of reality by excessive or disproportionate deformations.

A more modern method of model acquisition is the image-based synthesis, or photogrammetry. This process involves the creation of a digital human model from the co-registration of separate still images taken of a human body that are then used to reconstruct a 3D model. This method often begins by evaluating the human silhouette from a set of angles encompassing all views of the body and subsequently extracting the relevant anthropometric information needed to formulate the model. While this method is undeniably cheap, and very technically accessible as it only requires a set of 2D images, the noise and dependency on the background of the subject are issues yet unresolved in this method.

Statistics-based model synthesis is the most recently emerged method for model generation as it requires a database of human models to begin with. As these databases have recently become available this method has seen an increasing amount of attention for a number of reasons. Utilizing a consistent mesh structure throughout the database enables the synthesis of new human models based on real models. This method retains a high level of accuracy while allowing new methods of shape exploration through various big-data analysis techniques such as Principle Component Analysis (PCA). These techniques will be discussed further in the following chapters as this method is the primary focus of this research.

Due to the respective advantages and disadvantages of these methods many modern modeling systems incorporate a combination of the above processes. To better describe these relative advantages, beyond comparisons of cost or technical accessibility, the term “reality” is often used. Intuitively, a digital human model with a low level of reality would inherently cause a defective design. To better describe the various aspects of a digital human model the term reality can be broken down into three primary components as follows: visual fidelity, anthropometric reliability, and biomechanical / physiological accuracy [Baek2016].

Reality in the sense of visual fidelity is, simply put, an indicator of how plausible a digital human model is according to a visual inspection. This focuses on the external shape with special attention to things such as the proportions between body segments, geometry of the body and the general appearance. As our perception of a human body shape is very ingrained, things such as the silhouette and detailed expressions on the model can have a significant impact on the determination of the reality of a given model. While this is typically subjective and hardly quantifiable, it undeniably plays a role in the evaluation of the reality of a human model.

In a much more quantifiable approach, anthropometric reliability analysis regards the comparison of the body sizes of a digital human model to the human population. Essentially, the anthropometric reliability is a quantification of the probability of a real human having the body size parameters of a given model.

Reality in a biomechanical and physiological sense is a more in-depth quantification of the models reality, focused more on the application than the structure of the model. In this case the term reality of the model is regarding the physics modeling of the human body shape. This can involve anything from the mechanical properties of the musculoskeletal structure, to the material properties of the soft tissues incorporated into the model.

Initial efforts at digital human modeling first emerged from the fields of computer graphics and digital arts. As digital human models came to be of interest their development was mostly driven by the needs of the multimedia industry, including applications in motion pictures, computer animations, and video games, etc. At this point, the acquisition process for a digital human model was quite crude and involved a large amount of tedious hand labor done by digital artists or computer graphics experts whose focus was entirely upon the visual fidelity of the model. This process was more akin to traditional art forms such as sculpting and painting than the modern methods. It was this need to bypass the tedious labor that initiated the development of the methods in practice today. It was not until significantly later that anthropometric accuracy became a concern with the modeling process of digital humans, and even then these approaches remained separate from any concerns for visual fidelity. The eventual combination of these efforts has led the field of digital human modeling to where it stands today, and with it an evolution in the design process. The capabilities of modern digital human models have enabled a new design methodology that has come to be known as human-centered design, capable of pre-fabrication ergonomic assessment and design exploration.

Human factors has become an increasingly essential part of product design, and as such CAD technology has experienced an evolution regarding human-centered application. To that end, various aspects of the human body shape have been the subject of many efforts to digitize, quantify, and mathematically delineate within CAD systems. This has granted manufacturers the ability to consider these aspects of the human form as a set of design variables regarding their product, then allowing assessment and optimization of the ergonomics and human-centeredness of their design in a practical, accurate, and systematic manner.

This concept of human-centered design is undoubtedly directly reliant upon digital human models that contain accurate information regarding the various relevant aspects of the human body shape. With an accurate model, however, the benefits are quite significant throughout the design process as outlined in Table 1. The use of these digital human models can result in a significant reduction in development cost and time, while additionally offering an improved level of ergonomic quality and user-friendliness.

Table 1: Roles of Digital Human Models in the modern CAD systems as outlined by [Baek2016]

▪ Design reference for the product customization
▪ Reachability, fit, and visibility assessment
▪ Comfort and fatigue analysis
▪ Zero-prototype simulation
▪ Virtual dummy
▪ Safety analysis
▪ Virtual fitting room/Virtual try-on
▪ Manufacturing simulation
▪ Factory layout planning
▪ Sports equipment improvement
▪ Sports performance analysis
▪ Rehabilitation device design
▪ Medical device design / surgical planning
▪ Etc.

In recent history the capabilities and accessibility of advanced computer simulations have increased dramatically. This increase in the use of simulation software has altered many things but few more so than the design process, with concepts like human centered design and ergonomic analysis playing an increasing role. With access to greater computer processing power the capabilities of many simulations have begun to outclass the digital models they were designed to analyze. This is especially true in the case of digital human models. In this thesis I intend to not only discuss the shortcomings of the current digital human modeling methods, but to additionally present an improved process that yields models of greater accuracy both anthropometrics and statistical representation.

The rise in computing power has coincided with, if not instigated, a growing demand for Big Data analysis techniques. With massive pools of data being collected in many diverse disciplines, both scientific and commercial, techniques to effectively and efficiently analyze the data are in high demand. This demand has been met by a collaborative effort from the realms of computer science and mathematics to tackle the challenges presented by high-dimensional data. To that end, many techniques have been developed for so-called Nonlinear Dimensional Reduction (NLDR) that strive to simplify big data to a more familiar and accessible form. In this paper I will present an application of these techniques to analyze full-resolution

digital human models with the intent to create a more anthropometrically accurate and statistically robust breakdown of the human body shape space.

The process of mapping the human body Shape Manifold, or design space, begins with the analysis of a sufficiently large sampling of the human body shapes. There are many ways to obtain these models, both directly and indirectly, which can be decomposed into four main categories: (1) Direct model acquisition / creation, (2) Template model-based scaling, (3) Image-based reconstruction (photogrammetry), and (4) Statistics-based model synthesis [Baek2012]. While the Direct model acquisition methods, i.e. 3D whole body scanning, are not the most accessible due to the need for expensive equipment and post-processing the resultant models are the most accurate in terms of resolution and visual fidelity. To best ensure the accuracy of our results, this paper will use a combination of techniques that play to the strengths of each methodology. The models analyzed in this paper are all 3D scans of real people that have then been parametrized via a template-based model scaling process to ensure compatibility with each other. By then applying various NLDR techniques an accurate and complete mapping of the shape space can be performed.

1.2 - Motivation and Applications

The current process for the statistical breakdown of the human body shape-space typically consists of a 1D projection of the sampled digital models with a rudimentary separation into variance based population segments. This method essentially implies that a single parameter is sufficient to describe the vast differences in human body shapes which is obviously a crude description. While more robust techniques have been applied, like Principle Component Analysis in the case of Baek *et al*. [Baek2012] , there have been advances in the capabilities of modern NLDR techniques that have not yet been applied to the mapping of the human body shape space. By utilizing these emerging techniques the human body shape space can be visualized more accurately and a more intuitive analysis of the shape can occur. This resultant increase in the anthropometric accuracy, coupled with a more robust representation of the population in general, will present advantages in many fields.

In the area of human-centered product design the accuracy of the human model in the simulation stage of the design process is crucial to the effectiveness of the final design. From garments to motor vehicle interiors the accuracy and accessibility of a simulation depends heavily on the human model being used in the design process. For these two examples, however, the requirements differ. In the case of garment design specific portions of the population are targeted, i.e. dimensioning clothing to fit each of the representative population segments. This requires an accurate segmentation of the population that accounts for the many

ways in which the human body shape can vary so as to provide representative models that adhere closely to the full range of the people they are intended to represent. This can be achieved with high-dimensional clustering analysis to separate the human body shape space into a specified number of segments. However, for the design of a motor vehicle interior it is the full scope of the variation in human body shape that is of interest. The ergonomic analysis regarding the operation of the vehicle has progressed beyond the comfort of the seat, for example, to include the accessibility of the supplementary controls available to the user. The designer must account for the widest range of human body shapes as possible to ensure that people from all body shape demographics can easily operate all the controls available to them. This serves to increase the profitability of a design by enlarging the consumer-base, and as such is of great interest. These ergonomic considerations are again heavily dependent on statistically robust and anthropometrically accurate human models to ensure the validity of any design stage simulations.

The increasing power of digital simulation has found many applications in the realm of academic research. With regards to bio-mechanical human kinetics simulations the accuracy and flexibility of the models used is essential to achieving accurate simulation results. Initial attempts at a bio-mechanically accurate ergonomics simulation, such as the Jack simulation project, were relatively crude in both modeling accuracy and the scope of their application. However, more recent simulation projects such as the SANTOS research group at the University of Iowa have managed to incorporate a musculoskeletal system into their digital human simulation engine for the purposes of calculating forces within the body and running predictive dynamics simulations. The Virtual Soldier Research group at the University of Iowa began the development of the SantosHuman software package in 2003 [Santos]. Santos utilized the progress made by the Jack system to make some breakthroughs of its own regarding the implementation of true physics-based predictive dynamics with their in-house generative human model (Figure 1), as shown in [Abdel-Malek2006], [Abdel-Malek2007], and [Marler2008].

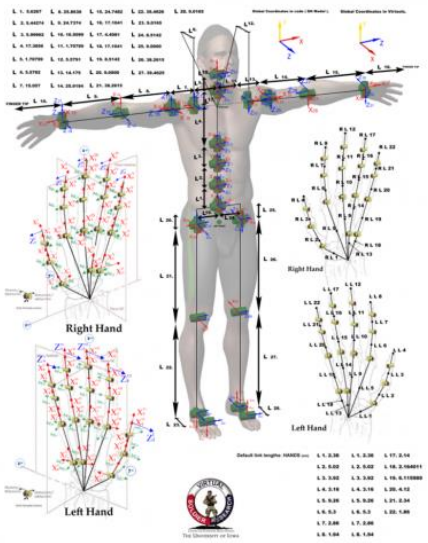

Figure 1: The skeletal system used by the SANTOS research project

The capabilities of Santos are currently unique in the scope of the considerations made by the simulation engine. The physics-based predictive dynamics solver uses validated mathematical models alongside novel optimization techniques to take into consideration the strength, fatigue, flexibility, balance, vision, posture, external forces, clothing, and equipment carried by the model while calculating posture and gait predictions. While this use of a generative human model is extensive, it is the physics based predictive dynamics that provides the true breakthrough nature as it does not rely on pre-recorded data, such as motion capture analysis, and as such can easily be altered an re-run for different conditions resulting in a more robust simulation capability. It is also interesting to note that the focus on the generative model used by Santos is not on increasing the reality of the model, but instead the functionality. By incorporating biomechanical models into their generative model framework they are able to go beyond the static stresses on the model and additionally focus on the long term dynamic effects of a given task with regards to the fatigue and hydration requirements that would be expected of a human. This adds an additional level of reality consideration that has only recently become a possibility in digital human simulation. Even these modern simulations, however, have little to no true flexibility with the diversity of their human models as they are dependent on consistent and compatible meshing structures. In this paper I present a novel approach to the generation of the human models to be used in these simulations that will eliminate the need for separately registered models. This then allows for an infinite set of digital models, within the range of feasible body shapes, which retain accurate and inter-compatible musculoskeletal systems and mass/inertial data essential to the simulation engines functionality. In addition to allowing the simulation engine to be used for the full scope of human body shapes, the process will generate more accurate models for each desired demographic.

In this way the range of the simulations applications in increased significantly as well as the resultant accuracy of the simulations.

Many databases of digital human body shapes have begun to emerge in recent history consisting of full body 3D scans such as the CAESAR, SizeChina, and SizeKorea projects. Access to these databases has, in turn, resulted in new possibilities regarding statistical and template-based human modeling methods that offer greater diversity and reality of shape than previous methods. To utilize this data the human body shape space must be mapped, often as a series of points in a high dimensional space. This requires a consistent meshing structure of the models being considered which can be obtained by a template-based parametrization of the models, as shown by Baek *et al.* [Baek2013]. This mapped space can then be regarded as the "Shape Manifold" for the human body space that offers a considerable number of advantages such as Manifold Enrichment and shape exploration, as outlined in Chapter 4.

Chapter 2: Related Works

The methodology discussed in this paper for the generation of digital human models can best be classified in the realm of example-based parametric modeling. The earliest example of a systematic approach to an example-based method was the work of Blanz *et al.* [Blanz1999], where the first human model database was established albeit only face scan data. This work was not only the first to develop a database of digitized humans, but also the first to approach the issue of compatibility between models. Obtaining their data with a 3D scanner resulted in a random sampling of the surface points, which were then resampled and reordered consistently thus guaranteeing compatibility between the face scans. As a result they were able to synthesize new face models in 3D by blending the geometrical data for different faces (Figure 2). To simplify this blending process they additionally performed a simple statistical analysis technique known as Principle Component Analysis, or PCA, to reduce the dimensionality of their data and allow for more direct and intuitive blending. This was the first instance of example based parametric modeling, a process that would be expanded upon greatly in the future.

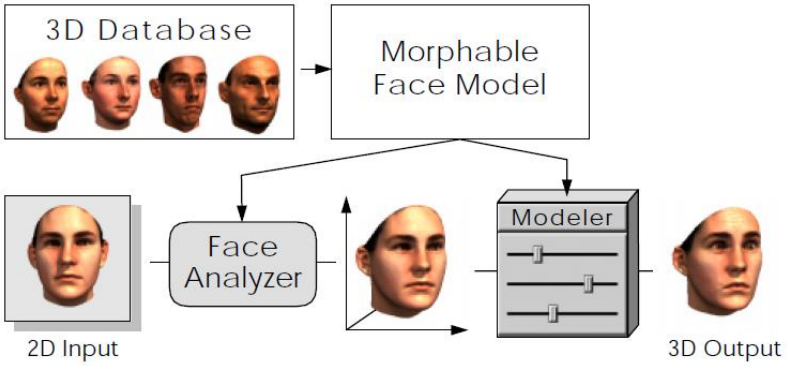

Figure 2: Human face analysis and blending process performed by Blanz et al. [Blanz1999]

Soon after, Allen *et al.* [Allen2003] took an approach very similar to that of [Blanz1999] in the application of this method to full body shape modeling. Using essentially the same overall framework, compatibility between the models was first established before proceeding to blend the models to synthesize new body shapes. The work of [Allen2003], however, made a significant contribution to the process by establishing a new method of guaranteeing the compatibility in a way much more suited to full body 3D scans. The noise, holes, and ambiguities inherent to full-body 3D scan data (shown in Figure 3) made the resampling method impossible to apply as it fails with incomplete scan data. To resolve this issue [Allen2003] manually prepared a template model by repairing and refining one of their scanned models and then proceeded to fit the rest of their models to this completed template model by minimizing the shape disparity. As a result they were able to efficiently recreate all of their scans without the noise or damage in the original data while simultaneously ensuring consistent geometry throughout their database of body shapes. This consistent geometry then allowed the blending of body shapes as described earlier as shown in Figure 4.

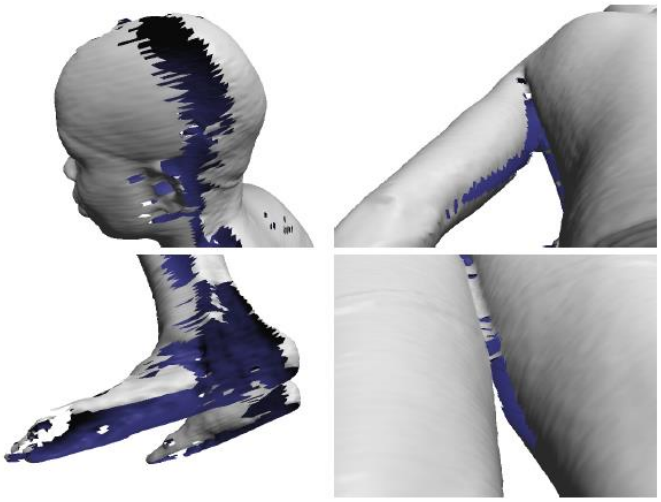

Figure 3: 3D scanned model used in the research of [Allen2003] displaying the noise and holes in the initial stages of model development

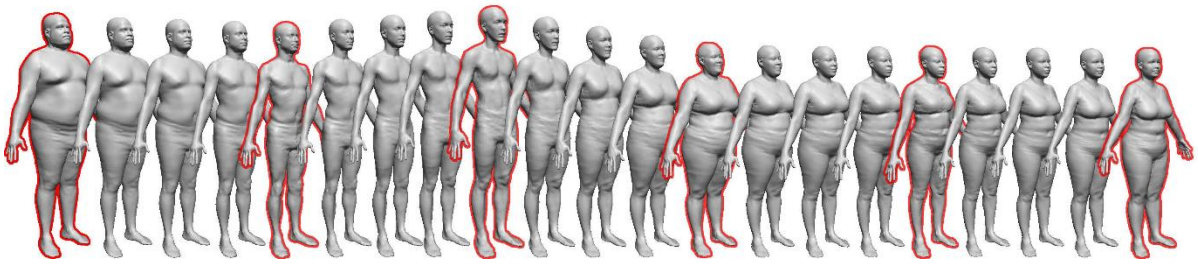

Figure 4: [Allen2003] Morphing between individuals. Each of the keyframe models (outlined) are generated from a Gaussian distribution in PCA space. These synthesized individuals have their own character, distinct from those of the original scanned individuals. The in-between models are created by linearly interpolating the vertices of the keyframes.

Due to the advantages presented by example-based methods they have grown to become the most common choice in human body shape modeling. The significant improvements offered regarding both anthropometric reality and visual fidelity compared to the other approaches has provided continuing incentive to many researchers. Additionally, the increasing capabilities and affordability of 3D scanning technology has contributed to the acceleration of this field, as evidenced by the similar works of [Anguelov2005, Park2006, Azouz2006, Allen2006, Xi2007, Zhou2010].

Capitalizing on the advantages of parametric modeling, Seo *et al.* [Seo223, Seo2004] established a new method of utilizing these parameters in a more intuitive manner. While methods such as PCA will extract parameters that can be used to adjust the body shapes, there is little intuitive meaning to the parameters. To resolve this Seo developed a more intuitive system of shape synthesis by adding weight functions to these parameters to relate them to body size inputs. This enabled a designer to more efficiently create a human model of the desired shape. Chu *et al.* [Chu2010] took a very similar approach by extracting critical information from a set of human models via PCA. This data was then correlated with various semantic parameters in a linear system of equations. As such, a new human body shape could be synthesized at an interactive speed through a linear regression process.

Wang *et al.* [Wang2005] had a similar idea, with the application focused more upon the garment design industry. In this research a parametric mannequin for a computer aided garment design system was formulated using human body shape statistics. By defining smoothly connected surface patches on the body with a set of feature points they were able to link surface modeling parameters with body size values, thus allowing users to model a digital mannequin by controlling the relevant body size values.

Recently, Baek *et al.* [Baek2012] progressed the idea of parametric modeling even further by developing a new framework for the translation of body sizes into blending weights. In this new framework a random set of body size values could be used, essentially allowing the user to neglect some parameters by

automatically determining their most natural setting based on the information provided. Additionally this proposed process would allow the use of non-metric inputs that would enable the development of a modeling system that could incorporate parameters such as age and annual income, etc.

Chapter 3: Mathematical Shape Descriptor

3.1 - Spectral Shape Representation:

Background:

As previously described, the implementation of a spectral shape descriptor can have many benefits and as such is an actively studied topic in fields ranging from computer graphics to finite element studies. With applications including shape retrieval, shape clustering, and statistical shape analysis, it is understandable that the topic is of great interest. The need for a sufficient method for spectral shape representation has only grown as well with the increasing file sizes and depth of databases of 3D models.

Deriving its mathematical foundation from spectral graph theory, the study of shape descriptors has seen much progress in recent years. Spectral graph theory makes use of the eigenvalues, eigenvectors, and eigenspace projections derived from carefully designed mesh operators that can then enable the capture of certain aspects of the shape as shown by Bruno Levy and Hao Zhang [Levy2010]. The earliest actualization of this concept came from the work of [Kac1966] entitled "Can one hear the shape of a drum?" This was the first instance of someone correlating the eigenvalues of the Helmholtz equation defined on a planar domain with the determination of the shape of the domain. In the following years, research in computational geometry revealed that this process could be extended to 3D shapes. However, it wasn't until advances in available computing power came to be in the late 1990's that this eigendecomposition of large sparse matrices began to draw much attention. Over the last decade this method of analysis has seen substantial growth as it has become more viable as well as useful.

The fundamental basis of spectral graph theory is quite similar to the analysis of vibration via the principle modes in acoustics or mechanical vibration. Spectral graph theory computes the principle modes of a shape for a given graph geometry and conducts an analysis of the shape using those principle modes [Baek2013]. To accomplish this, a differential operator is defined for the graph so that the desired properties of the analyzed geometry are extracted to the subsequent eigendecomposition of the graph operator. The operator typically selected is the Laplace-Beltrami operator (LBO) which is a Laplace operator generalized on a Riemannian surface. This operator can then be geometrically interpreted as a curvature normal with a vector magnitude equal to the curvature. With this inherent relation to the first and second order local differential geometry it is easily imaginable that the operator then includes sufficient information to describe the entire surface geometry.

Due to its formulation the LBO offers many advantages in that it is isometrically invariant, as well as being easily made to be scaling-invariant, all while being relatively easily computed. The ability to compress a shape to a desired number of dimensions presents a number of advantages as well as it retains the intuitive geometric information as shown by the work of [Reuter2006]. Due to this, the Laplace-Beltrami spectrum has found uses in shape retrieval and matching [Reuter2005; Ovsjanikov2009; Bronstein2010], shape segmentation [Reuter2009a; Fang2011], posture-invariant correspondence matching [Mateus2008; Dubrovina2010], and statistical shape analysis [Niethammer2007; Reuter2009b; Shi2009].

Requirements:

For the purposes of this research we will focus on the statistical analysis portion of the potential applications, and as such we must define the required properties of a spectral shape descriptor. Essentially, a shape descriptor should properly characterize a complete shape with a reduction of dimensions, while retaining sufficient ability to discriminate between shapes based on a continuous dependency on the shape change. In this way one can then separate different shapes and measure then disparity between them. The outline of the full requirements, as outlined by [Baek2013] and [Reuter2006], is as follows:

1. **Isometry-Invariance**

   A shape descriptor should not be affected by basic manipulations such as translation, rotation, or even posture change to remain truly invariant under isometry.

2. **Parametrization independence**

   To ensure global applications the shape descriptor must be independent of the mesh parametrization. As a single shape can have an infinite number of parametrizations it follows that a shape descriptor should be capable of defining the shape regardless of the parametrization.

4. **Linear proportionality to the most isometric deformation**

   A shape descriptor should also vary continuously with respect to the change of a shape. With the most isometric deformations of the model the descriptor should vary linearly, thus adding a direct capture of the discrepancy between shapes. Considering the blending of two models as the most isometric interpolation the shape descriptor should be linearly proportional to this change, thus enabling a linear algebraic interpolation of the shape descriptor in the exact fashion of the interpolated model.

5. **Dimension reduction**

   Considering the large, and increasingly so, size of scan data any statistical computation requires significant computing power. To this end, a shape descriptor of minimal dimension would enable much more efficient analysis procedures.

6. **Efficiency**

   Similar to the foundation for (4), the computation of the shape descriptor should be accomplished with a minimal processing load.

7. **Depictiveness**

   The descriptor should offer some intuitive meaning, e.g. some geometric / physical interpretation should be obtainable from the shape descriptor.

By using the above properties one can then judge the efficacy of a spectral shape descriptor. Additionally, they will be used to justify a modification of the LBO formulation as outlined in the following section.

3.2 - Laplace – Beltrami Operator:

Formulation:

To begin the discussion regarding the formulation of the LBO some context must be given as to what the spectrum of a shape represents. Consider a surface as being in a paused state of membrane vibration. This surface can then be modeled as a stationary wave, to use a term from acoustics and mechanical vibration theory. Such a membrane was first analyzed by Chladni in 1787 when he experimented by vibrating a sand-covered metal plate (Figure 5) to observe the resultant patterning in the sand. When such a membrane

vibrates certain areas remain still though the vibration, resulting in a collection of sand in these areas. This process can be modeled through the Helmholtz equation as shown in equation 3.1 below:

$$\Delta f = \lambda f \tag{3.1}$$

where Δ represents the LBO, defined for a C_2 continuous real-valued function f defined on a Riemannian manifold M as follows:

$$\Delta f := div(grad(f)) \tag{3.2}$$

where grad and div denote the gradient and divergence on the manifold M, respectively [Baek2013].
Then, the LBO can be locally parametrized on the manifold to the form below:

$$\Delta f = \frac{1}{D}\sum_{i,j=1,\dots,n} \partial_i\left(g^{ij} D \partial_j f\right) \tag{3.3}$$

In this formulation g^{ij} is the (i,j)th element of G^{-1}, where G is the metric tensor with elements defined as g^{ij} $:= \langle \partial_i \Psi, \partial_j \Psi \rangle$, with Ψ derived from the parametrization $\Psi : \mathbb{R}^n \rightarrow \mathbb{R}^{n+k}$ of the submanifold in $\mathbb{R}^{n+k}$ space. Additionally, D represents the determinant of G. This formulation of the LBO is essentially a mapping of the local curvature and deformation of a surface from local space to a global space. This curvature information is then summed and normalized for a conversion back to the local reference frame.

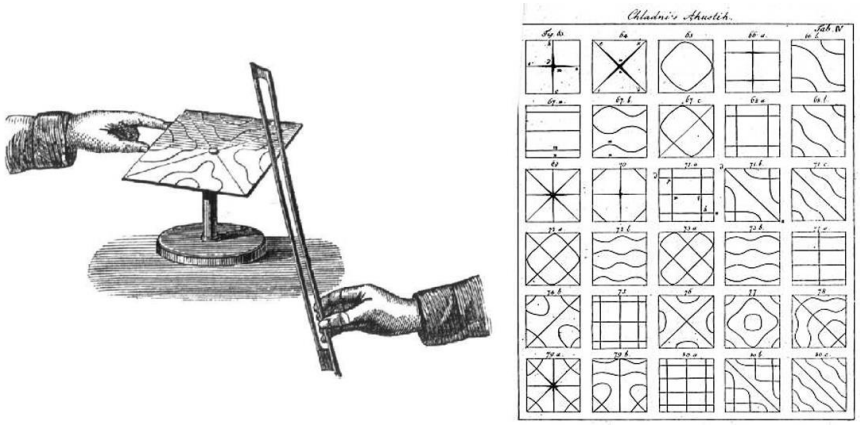

Figure 5: Chladni's vibrating plate experiment

The eigenvalues of the above operator then correspond to the shape information based on the local curvature information. Therefore, the spectrum of these eigenvalues presents a spectral shape descriptor that, in a continuous case, satisfies all of the above requirements. As the operator does not change without an adjustment to G in equation 3.3, it can be seen that it is invariant under isometry. Additionally, due to the linearly dependent nature of the LBO on the elements of the metric tensor G the desired linear

proportionality is also achieved. The remaining requirements can be shown to be satisfied by the proofs completed in the work of Reuter *et al.* [Reuter2006].

Modification & Discretization:

This method is not without its problems in practical applications, however. When discretizing the domain in question a certain amount of error is developed. While multiple discretized forms have been developed, the discretized formulation of the LBO for a triangular mesh developed by Meyer *et al.* [Meyer2002] has become a standard in many applications. The work of Baek *et al* [Baek2013], however, showed a significant improvement in the reduction of the errors developed by the discretization. In their research they defined a new linear operator that, while quite similar to the LBO, focuses more upon the preservation of local lengths for its spectrum computation as shown below:

$$(\Delta f)(v_i) = \langle \Delta f, 1_i \rangle = \sum_j \frac{l_{ij}}{|e_{ij}|^2} (f(v_j) - (f(v_i) \tag{3.4}$$

where 1_i is the Dirac's delta function that is defined on the discretized mesh in question and has a unit value at vertex *i* while remaining 0 at all other vertices. Additionally, e_{ij} is the edge length between vertex *i* and *j*. As can be observed from above, the properties of the operator depend upon the definition of l_{ij}. To capture metric changes during deformation in a precise manner, l_{ij} is set to be $|e_{ij}|/\deg(i)$, where deg(*i*) denotes the number of outgoing edges. In this way, the operator is directly dependent in the metric of a surface as outlined in [Baek2013]. With this formulation the operator retains all the desired properties as outlined above, and for purposes of distinction from the LBO will be referred to as the Metric Dependent Signature (MDS).

Comparison of Methods:

The advantages of this reformatted version of the Laplace-Beltrami operator are easily made apparent when comparing the spectrums of a set of isometric models, subjected to various posture changes. As isometric-invariance is a desired quality of the operator it is imperative to check this, although true invariance is not possible with a discretized version. As the models analyzed (shown in Figure 6) are all isometric versions with a varying amount of posture change the spectral results of the LBO and MDS can be compared in Figure 7.

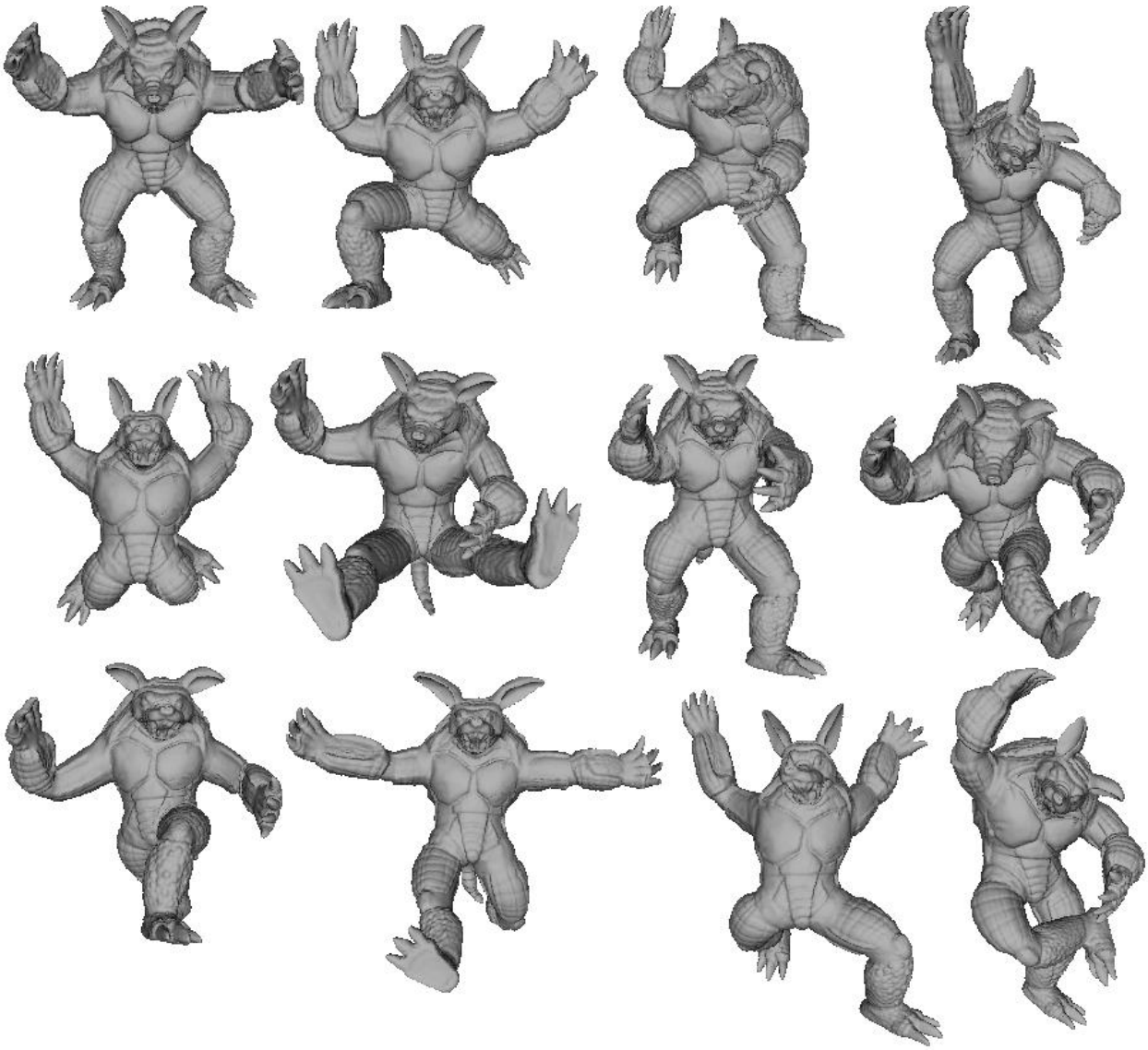

Figure 6: Sample of the isometric models subjected to posture change for comparison of spectral operator results

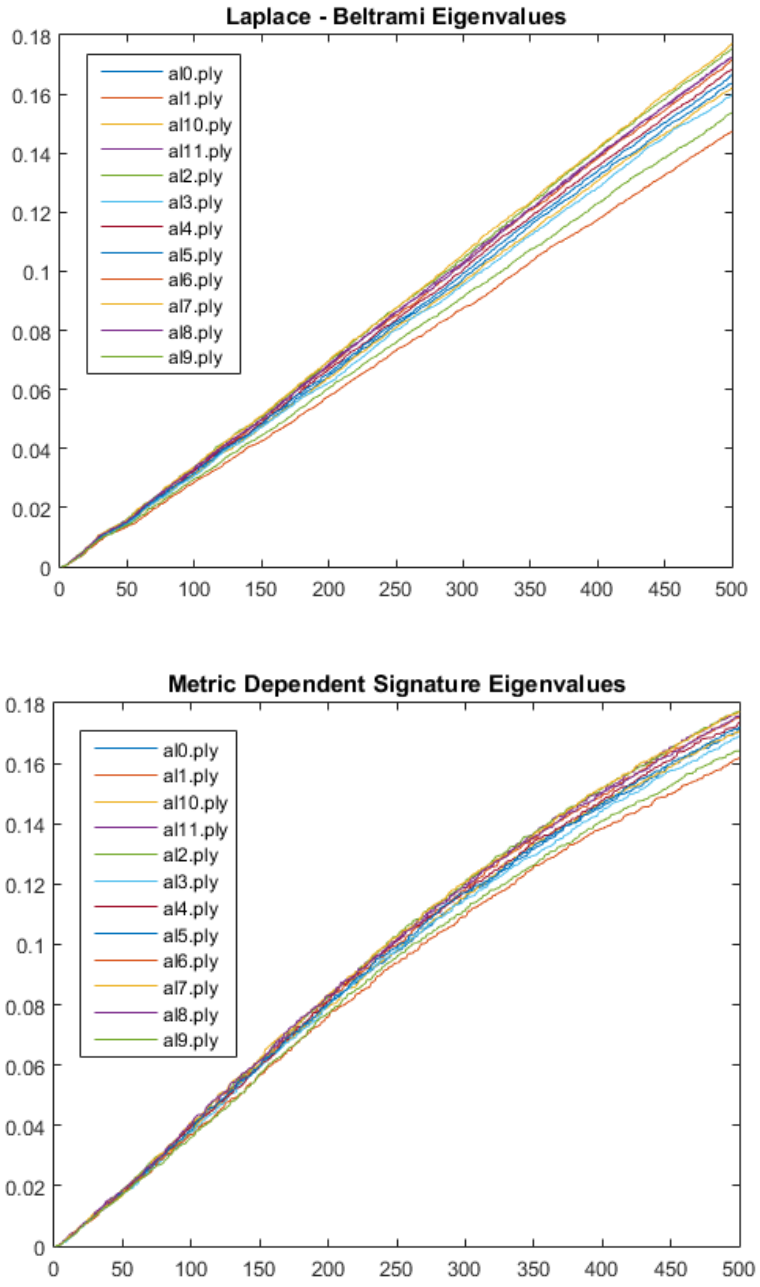

Figure 7: (Top) - Laplace-Beltrami spectrum as calculated from the formulation presented by Meyer et al. [Meyer2002]; (Bottom) Metric Dependent Signature Spectrum formulation presented by Baek et al. [Baek2013] Note that the lack of divergence in the higher end of the spectrum shows the desired improvement in isometric invariance

As can be observed from the figure above, the results show a significant improvement in the isometric invariance with the Metric Dependent Spectrum. The results of the spectrums, especially in the range of the 200th to the 500th eigenvalue, show a greater level of consistency across the models. As outlined by Baek *et al.* [Baek2013] it is sufficient to limit the number of eigenvalues in the spectrum to the 300 to 500 range when applied to human models as the details of the model are sufficiently captured.

Result:

The use of this spectral shape representation offers a significant amount of benefits. In this research the most advantageous aspect, however, is the reduction of order in the representation of the shape. This simplified shape characterization allows for a much more efficient clustering and analysis of the data, as outlined in the later chapters.

This formulation of spectral shape representation was applied to the set of models developed using the Santos template (the process for which can be found in Chapter 5) and can be found below in Figure 8. As can be observed, the spectrums show similar trends as the shapes are all within the scope of the human body shape. The differences, however, are represented by the differences in the spectral values to an increasing extent in the higher range of values. This is to be expected as the initial spectral values will be quite similar across the range of human bodies, indicative of the fact that each body has the same topology and general structure. The differences in the shapes of the body segments then begin to take a larger effect in the later spectral values.

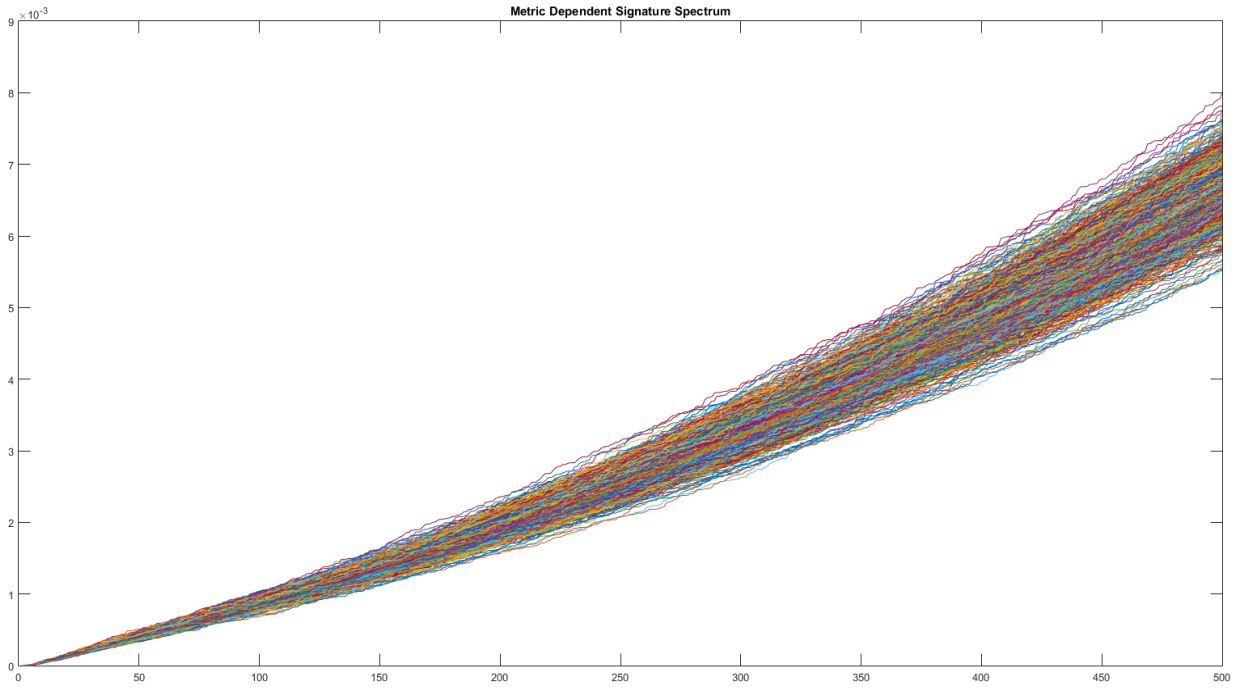

Figure 8: Metric Dependent Spectrum calculated for the set of Santos Morph models generated from the CAESAR dataset

Depending on the origins of a model, and its intended application, it can be quite common for a digital human to be composed of a number of meshes. This is often done for purposes of texture mapping or to allow movement of a body part independent to the rest of the body, e.g. the rotation of the eyeballs. These multiple meshes can cause some discontinuities in the mesh when considered as a whole human structure than then leads to a singular matrix when calculating the spectral representation, resulting in infinite or poorly scaled values. To resolve this a random sampling method was implemented to sample vertices from each of the meshes that make up the body. By using a brute-force approach that ensures a low variation in the distance between sampled points the level vertex density in each of the meshes was made irrelevant. As can be imagined, the mesh for realistic hair on a model would be much more refined than the section for the torso. This increased mesh density would then skew a random sampling to consider the head more than the body which is, in fact, the opposite of the desired result. By enforcing a minimum distance between sampled points this can be avoided and the complete human body shape can be represented by a simplified sampling. The spectral results for this improved sampling method can be found below in Figure 9.

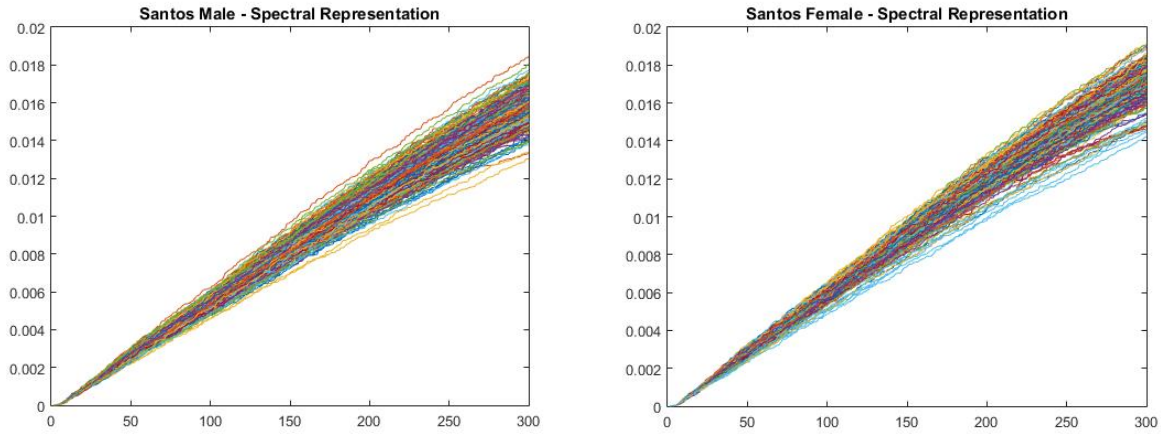

Figure 9: Spectral representation of the digital human models (Left-Male, Right-Female) generated by template fitting a 3D body scan database to the SANTOSHUMAN avatar using the improved random sampling method to account for the separate meshes and mesh density disparities.

This new sampling method allowed for a reduction in the number of eigenvalues required to describe the human body shape as the results were more accurate due to the removal of the bias towards the head / hair. This improved point sampling method is then referred to as the Power Spectrum, in credit to the power series method of the brute force point testing.

Chapter 4: Shape Manifold Theory

Shape Manifold Theory is a relatively new method of conceptualizing shape and design from a mathematical perspective. While high-dimensional mathematics has existed for decades it was not until recently that computing power allowed for the generation of high-dimensional digital representation of complex shapes in abundance. As a result, new methods have been generated to visualize and arrange this data, among them Shape Manifold Theory (SMT). As high-dimensional data clustering methods improve, the functionality of SMT does as well, as it is essentially a clustering of similar shapes represented as points upon a high-dimensional manifold as outlined further in the following sections.

4.1 - Mathematical Definition of Shape:

Shape Parameters:

In order to discuss the application of shape manifold theory (SMT) to this research, a preliminary review of the theory is required. The initial step in this is to discuss the mathematical representation of a shape. When considering an object, be it a chair, a car, or the human body, once can imagine a set of *shape* (or *design*) *parameters* that determine the shape of the object. Expanding this with the human body, measurements such as the height, chest and waist girth, and shoulder breadth etc. could be considered as the set of shape parameters required to describe the shape of the human body. These shape parameters are, by their nature, metric properties. As such, any applicable variable defined by Euclidean metrics, e.g. lengths, areas and volumes, can be considered shape parameters. Additionally, geometric properties such as circumferences, geodesic lengths, and absolute curvatures can also be considered. While the possible shape parameters are diverse, they are restricted to purely metric properties so as to exclude things such as price, weight, and age. This exclusion forms the distinction between *shape parameters* and *design parameters*.

Cardinality of Shape Parameters:

Intuitively, as the complexity of a shape increases the number of shape parameters required follows suit. The number of parameters is not necessarily finite either. Given the context of an object the number of shape parameters required may grow to infinite levels. It is easy to imagine a finite set of parameters capable of completely describing the shape of a simple object such as a bolt or a gear, or even more complex mechanisms such as a bicycle. However, more complex shapes such as the human body may require an

infinite set of parameters for accurate representation. At a high enough level of detail this is quite understandable. Consider, for instance, the cardiovascular system within the body. The dynamic cross-sectional profile of each of the incredibly numerous blood vessels would require an incredibly complex set of parameters to be sufficiently represented. When additionally considering the remaining metrics such as the varying, and non-symmetric, thickness of the vessels the amount of parameters required grows exponentially. Expanding this process to encompass the entirety of the human body is becomes quite easy to conceive the infinite scope of the parameter set required.

4.2 - Applied Shape Manifold Theory:

With all the necessary shape-definition concepts now defined we can discuss the mathematical definition of a shape. Mathematically, the shape of an object can be considered as the topology of an object that is then equipped with shape parameters at each node and connectivity information along each edge. The shape parameters at each node are then the necessary metrics that can accurately and completely describe the shape of that particular segment represented by that node. The connectivity information then provides the relative position and orientation information necessary to assemble the segments. Therefore, a shape can be completely reconstructed from a fully connected and completed graph.

This definition of a shape is, however, not very practical in this form as infinitely many topologies may exist for objects of the same context. For an example of this, consider a tree as each tree will have a significantly different topology even within the same species. While impractical, this formulation provides the foundation for more useful applications of SMT.

Space of Shapes:

Considering the exterior shape of the human body one can conceive a finite, albeit large, set of parameters required to fully describe the shape. The number of parameters required can then be considered the dimensionality of the shape. Let us then consider a non-negative, real Euclidean space of the same dimension. The human body shape described by the aforementioned parameters then forms a point in this space. This high-dimensional space is then referred to as the *embedding space* for the human body, as it contains the ability to fully represent a human body shape as a single point. By tweaking the shape parameters one can easily conceive new body shapes that would then form a separate point in the embedding space. Expanding this idea, a collection of human body shapes would then form a "thin" subspace within the embedding space. While the embedding space has no limitations on the proportions of these parametric

adjustments we can consider a range of plausible human body shapes being mapped within the embedding space. This plausible subset of the embedding space is then denoted as the *shape space* for the human body.

This human body shape space, or *shape manifold* is then defined as the subspace of a high-dimensional embedding space that contains all plausible human body shapes. This shape manifold forms a nonlinear subspace of the embedding space that can offer methods with which to explore the human body shape. For example, one can imagine that two similar body shapes would be relatively close to each other on the shape manifold. For two very distinct bodies, however, the distance may be quite large. This distance then has some intrinsic meaning that can be understood and manipulated. When considering (theoretically) singular adjustments in body shape, e.g. fat to skinny or short to tall, the transition between the shapes can be represented as a geodesic path along the shape manifold surface. Each point along this path represents a separate plausible human body shape that transitions in a specific manner along a particular path. To this end, one can imagine a "direction" along the shape manifold that represents various parameters such as height or waist girth.

A truly singular adjustment would be represented by a Euclidean vector in the embedding space, however, as the shape manifold is non-linear this would cause a divergence from the shape manifold. This is intuitively due to the fact that the human body does not simply change with regards to a single parameter without corresponding adjustments to the others. By taking the geodesic path along the shape manifold it is ensured that the relative proportions of the shape parameters continue to form a plausible human body shape, while still allowing exploration through the various shape parameters.

Chapter 5: Body Shape Manipulation & Shape Space Enrichment

5.1 - Problem Statement: Application to SantosHuman

Given the advances in the reality of digital human models, and the resultant analysis capabilities they present, many research groups have turned their focus to the simulation engine side of the problem. By simply obtaining a handful of models, they can then implement a full musculoskeletal structure within the body that allows the calculation of joint torques *etc*. Some groups, however, such as the SantosHuman research group at the University of Iowa [Santos] have managed to progress this research by additionally considering some long-term biological effects. Their research has allowed for the consideration of strength, fatigue, flexibility, balance, vision, external forces, clothing / equipment carried, *etc*. to name a few. This information is then used for the "posture prediction" analysis, as well as "predictive dynamics" that takes the force / inertia data from a Kinetics and Dynamics standpoint to generate the resultant Kinematic information. While this is a novel process for dynamic human modeling, they remain quite limited in the extent of the models that are available. This is due to the fact that each additional model must be fitted with a skeletal structure (Figure 1) and subsequently have the mass and inertial information calculated for each body segment. With no correlation between the models this process becomes a tedious one involving a significant amount of both time and expertise in digital model manipulation.

In this research I present a method capable of bypassing this step by developing a "dynamic" model capable of being adjusted throughout the spectrum of human body shapes, while maintaining the internal structure and inertial information critical to their analysis procedures. By using their standard Santos model as a template model and deforming the template to match the body shapes represented in the CAESAR (Civilian American European Surface Anthropometry Resource) database a set of models can be generated that maintains the same connectivity information and general mesh structure of the original Santos. This dataset can then be clustered, using the methods described in the following chapter, to map the Santos model set.

5.2 - Parallel Transport of a Shape:

While advances in 3D scanning technology has led to an increase in the amount of available models, the shape space still consists of a discrete sampling of the body shapes in the vast majority of applications. This can lead to difficulties in obtaining a model of a specific shape and size. However, once some representative vectors along the shape manifold have been identified for a given population they can be used to enrich the shape space for a specific human model via a parallel transport process.

First, let us consider the shape manifold for the human body as a surface in high-dimensional space. As this space contains all feasible body shapes it is natural to image the progression of certain metric aspects of the human body shape when moving in a constant direction along the shape manifold surface. For example, a particular direction may represent the height of the model, another direction the shoulder girth, *etc.* By extracting these vectors, via the methods outlined in the following chapter, one can use them to enrich the shape space for a particular model. This is where the concept of parallel transport becomes relevant. By transporting the high-dimensional vector for a particular body shape metric to a specific model one can then apply that change to the model by moving the point along the vector.

In this way, one can enrich the shape space for a particular model infinitely by generating new models along the metric vectors that have been transported to the model in question. As these vectors simply represent a change of position for the vertices of the model the mesh structure and connectivity remain unchanged. This method of shape space enrichment not only affords the designer an infinite set of models with intuitive control over the shape, but also guarantees compatibility between the generated models.

5.3 - Results:

Template-Based Model Generation:

As outlined in the previous sections, one of the most popular human body modeling methods is the so called template-based modeling. By using a completed model as a template, and subsequently deforming the template to fit 3D body scan data a model can be efficiently generated. Not only does this process eliminate the need for prolonged post-processing but also generates models with a consistent mesh structure and connectivity.

Once provided with the human model used by the SantosHuman [Santos] research group, this process of template-based modeling could be applied. By using the Santos model as a template and deforming it to the scan data from the CAESAR dataset a new set of models could be generated that were compatible with the original Santos application. This was accomplished by applying a Non-Rigid Transformation process to the template model. This transformation was done by implementing the standard H-Anim markers [H-Anim] on the template model and scan data, and registering them together. Using the Gauss-Newton method a solution could be obtained in a way that allows for a variation of weights for the different markers as things like the orientation of the hand are of less import than matching the shoulder width, for example. An example of this registration process can be found in Figure 10. The H-Anim markers can be seen in the red and green, while the two models are in yellow (template) and blue (scan data).

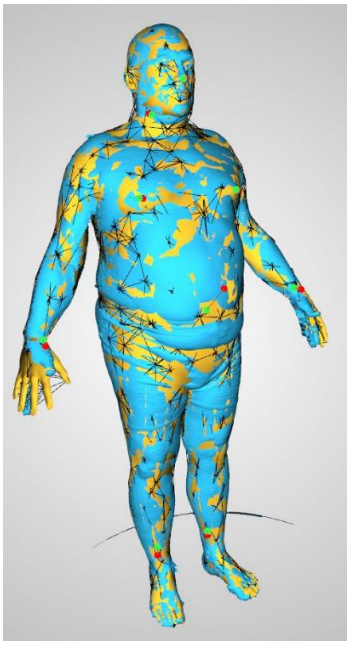

Figure 10: H-Anim markers being used for the registration of a template model to a human body scan

Enrichment of Santos Shape Space:

Using the process detailed above, the Santos model (Figure 11) was deformed to create a set of human models with various body shapes compatible with the original model (Figure 12). As these models were created by deforming the original Santos in a uniform manner they posess the same mesh structure.

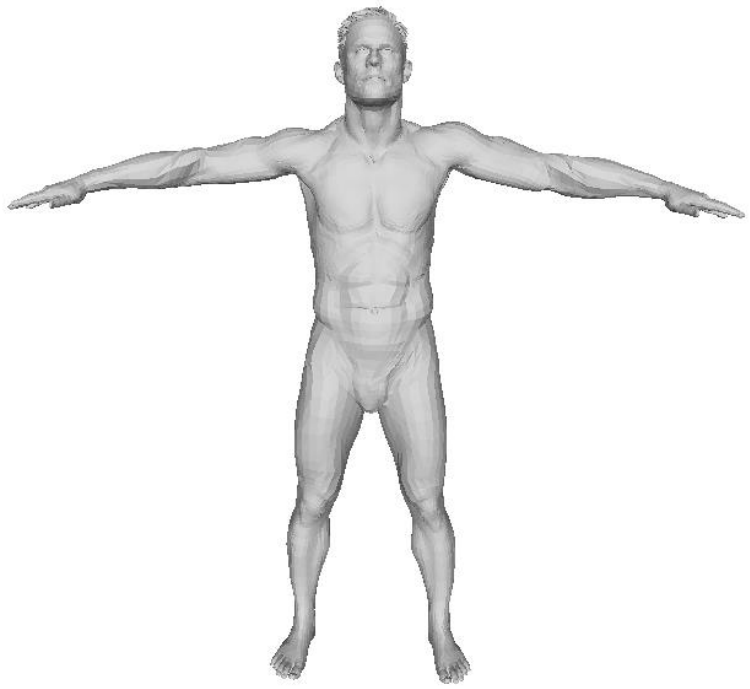

Figure 11: Original Santos model used as a template for the template-based model generation

While some of the target models for the template deformation were female, the Santos original model was still used as the template. As a result the facial structure was given lower weights in the transformation process to prevent any extreme distortions in an area with a high sensitivity regarding visual fidelity. Additionally all of the Santos morph models share the same "haircut" as the purpose of this research was with regards to the shape of the body.

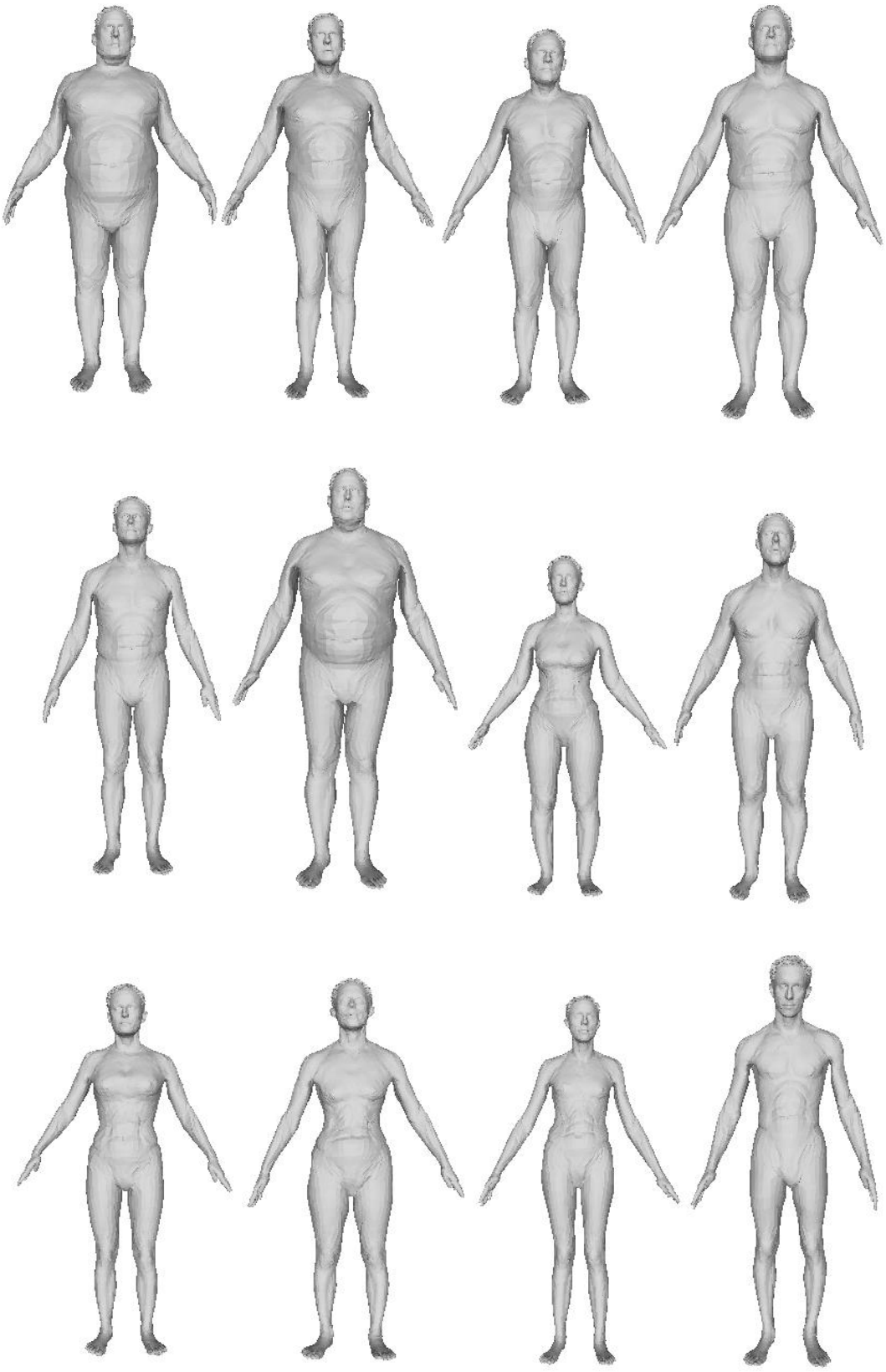

Figure 12: Santos template-morphs across the range of both male and female body shapes

As can be observed from the figures above, the resultant models maintain a high level of reality across a wide spectrum of body shapes. However, the models shown above are just a sample of those created. To illustrate the body shape space enrichment a reduced-dimensionality plot of the shape manifold was generated using the Sammon Mapping technique (Figure 13). While many other dimensionality techniques will be explored in the following chapter, the Sammon Mapping method generates a nice 2D approximation of the shape manifold for this application. The Original Santos model is represented by the enlarged red point, while the surrounding purple points all represent template-based morphs similar to, and including, those shown in Figure 12.

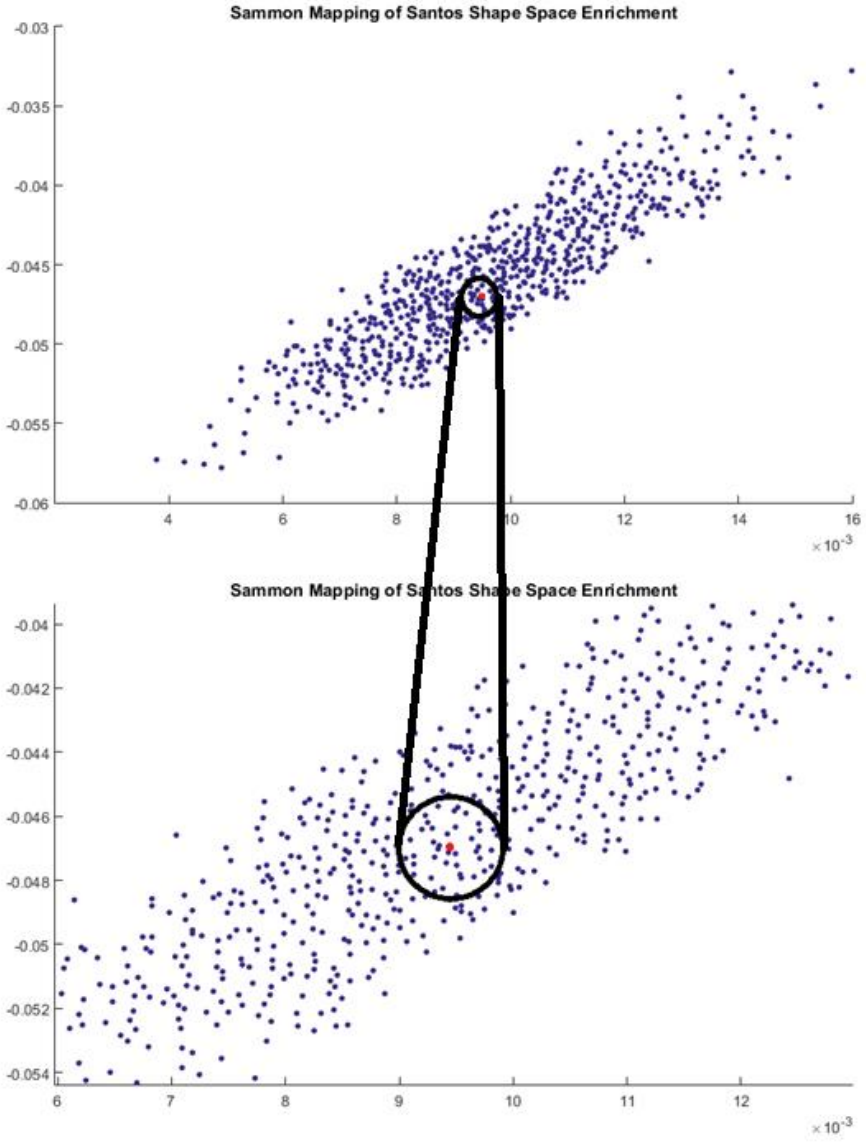

Figure 13: Detail of Santos Shape Space Enrichment with the red point representing the original Santos model and the purple points representing the Santos Morphs generated by the template-based modeling process

The models shown in the plots above are represented by an application of the Sammon Mapping dimensionality-reduction technique applied to the spectral data calculated for each of the generated models. As such, the models arrangement on the plot has an inherent meaning derived from the spectral representation process. For example, short models and skinny models will be on opposite ends of the plot from their tall and overweight counterparts. This makes intuitive sense regarding the seemingly Gaussian distribution indicative of the greater abundance of models near an "average" body shape, as opposed to more drastic shapes. However, the linear appearance of this dataset is in part due to the process of the Sammon Mapping algorithm which will inherently linearize a dataset to some degree.

This "spectral-based" body shape clustering is much more efficiently observable than attempts based off of the mesh structures themselves. This then enables the statistical shape clustering analysis discussed in the following chapter.

Chapter 6: Anthropometric Human Models Based on Population Analysis

6.1 - Problem Statement:

The increasing incorporation of digital human models into the design process has fueled the advancement of modeling technology and methodologies, resulting in human models with a high level of reality. However, the subsequent analysis techniques required to fully utilize these models are often crude when compared to the models themselves. The recent development of large databases of human models has enabled some novel solutions to these problems, at the forefront of which is unarguably the means to accurately represent the full extent of human body shapes with a reasonable number of representative models.

Early efforts in digital human modeling were primarily focused on the accurate capture of a specific human body shape that maintained a high level of reality. However, recent market demands are less interested in this aspect but rather a set of models that fully represents the entire human population. This has many obvious applications from ergonomic analysis to the garment industry, where statistically generated representative models could be used as the standard for garment design shapes.

The incredible amount of diversity in the human body shape has made the process of representing the entire spectrum of body shapes with a reasonable number of representative models a complex task. While representative models have been generated before [CadHuman; Hu2012], the methods used are generally crude and oversimplify the diversity of the shapes. A typical assumption made in these attempts is the linearity of the human body shape space, which causes an inherent error in the generation of any representative models. This research presents a method to correct this error by accurately mapping the human body shape space, and subsequently performing a cluster analysis capable of dealing with the non-linear high dimensional shape space. Once identified, these clusters of models can be used to generate an averaged model that then represents the cluster it was derived from. As a result, an improved set of representative models can be generated that ensures that any given body shape is closer to its representative model on the human body shape manifold.

6.2 - Visualization of Shape Manifold:

Big-data analysis has quickly become a growing field in recent history as the number, and size, of databases being generated continues to grow. As a result, many dimensionality reduction techniques have been developed to help visualize these high-dimensional data. Of particular interest in this research is a method to identify the natural clustering of the human body shape data so as to define and generate the appropriate representative models.

There are many techniques available for this clustering analysis that each involve different methods to recreate the high-dimensional structure in a domain of a specified dimension. These methods can be found in Table 2. Due to the different approaches taken in the methods they produce different results when applied to a database of digital human models. As many of the methods focus on recreating and approximating the local linearity of the data the results can also depend heavily on the extent of the neighborhood considered, e.g. how many nearest neighbors to constrain.

Table 2: Common Dimensionality Reduction methods used in the literature for digital human analysis and Big-Data

1. Principal Component Analysis (PCA)	15. Diffusion maps
2. Probabilistic PCA	16. Neighborhood Preserving Embedding (NPE)
3. Factor Analysis (FA)	17. Locality Preserving Projection (LPP)
4. Classical multidimensional scaling (MDS)	18. Linear Local Tangent Space Alignment (LLTSA)
5. Sammon mapping	19. Stochastic Proximity Embedding (SPE)
6. Isomap	20. Deep autoencoders (using denoising autoencoder pretraining)
7. Landmark Isomap	21. Local Linear Coordination (LLC)
8. Local Linear Embedding (LLE)	22. Gaussian Process Latent Variable Model (GPLVM)
9. Laplacian Eigenmaps	23. Stochastic Neighbor Embedding (SNE)
10. Hessian LLE	24. t-Distributed Stochastic Neighbor Embedding (t-SNE)
11. Local Tangent Space Alignment (LTSA)	25. Neighborhood Components Analysis (NCA)
12. Conformal Eigenmaps (extension of LLE)	26. Maximally Collapsing Metric Learning (MCML)
13. Maximum Variance Unfolding (extension of LLE)	
14. Kernel PCA	

Initial Investigation – SizeKorea Database:

The initial step in the process of mapping and clustering the human body shapes is to investigate the clustering methods available to identify those best suited to the mapping of a database of digital human bodies. As a test case for the identification of this optimal method a smaller set of digital human models was used. The SizeKorea database, consisting of 108 male and 98 female models, was analyzed with a variety of the dimensionality reduction methods available. As some methods allow for a manual selection of the number of neighbors considered for the local linearity consideration an additional investigation was performed in this regard.

Due to the many ways in which the shape of the human body can vary a linear projection of the data points is not desirable. Instead, a more natural collection of clusters is of more use, although some overlap in these clusters will be unavoidable.

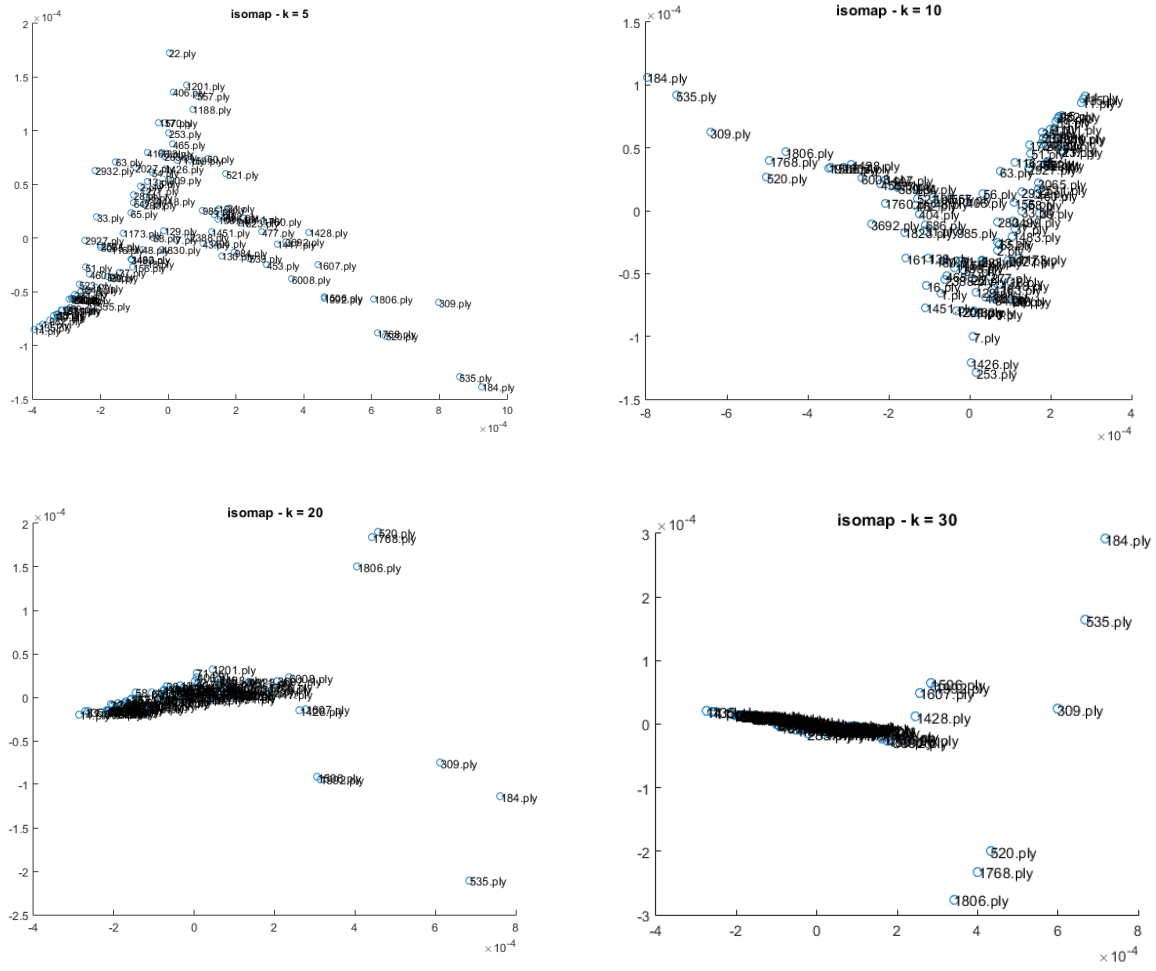

Figure 14: Isomap dimensionality reduction analysis of the SizeKorea male model database with the number of neighbors considered (k) ranging from 5 to 30, plotted alongside are the corresponding file names used to check the distribution of the models.

As can be seen from the figures above, the number of neighbors considered can have a drastic effect on the resultant clustering when using the Isomap method. This effect, however, is not universal. When comparing the above Isomap (Figure 14) results to those of the Local Linear Embedding (LLE) method (Figure 15) the effect of the "k" specification is shown to have the opposite result. This is due to the differences in how the algorithms attempt to recreate and preserve the neighborhood information of the data points.

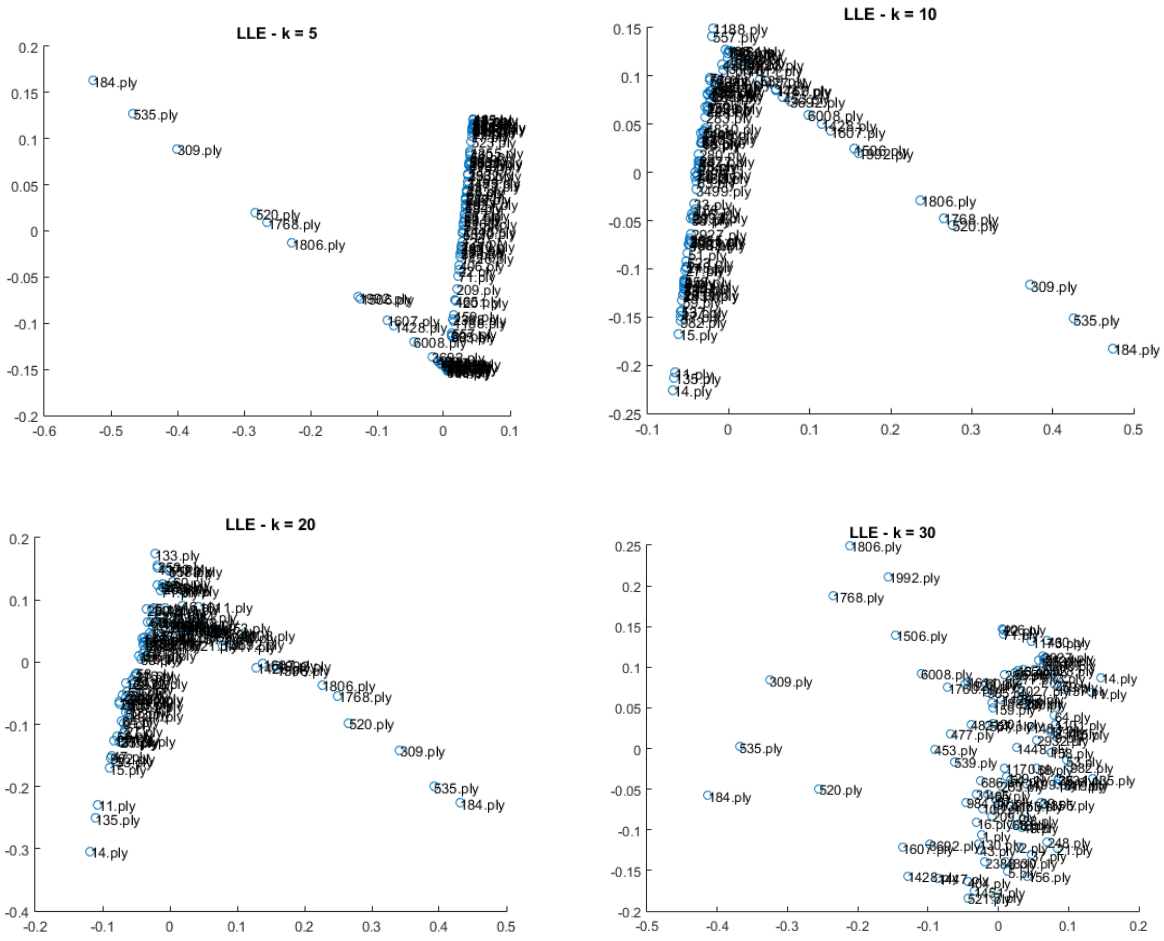

Figure 15: Local Linear Embedding (LLE) dimensionality reduction algorithm applied to the SizeKorea Male model database

The Local Linear Embedding technique takes a specified number of neighbors and attempts to recreate the relative distances of the neighbors in the desired dimension. By incorporating a larger neighborhood the natural clustering of the data could be better maintained, although the outlier nature of some of the body shapes is visually increased. From the initial investigation of dimensionality reduction methods it is quite apparent that these methods are quite sensitive to the parameters used, primarily the number of neighbors considered. This may be due, in part, to the general similarities of the models in that they share a common topology as a human body shape.

6.3 - Clustering and Statistical Shape Analysis – Santos Morph Data:

Once the Santos Morph dataset was created, as outlined in the previous chapter, the spectral analysis was computed with the Metric Dependent Spectrum (Figure 8). Using this spectral information, a cluster analysis was performed on a concatenation of the spectral data for the entire set of body morph shapes. This analysis assigned each of the morph shapes to one of six total clusters, as six was deemed a practical number for a statistical representation. To visualize this clustering, the dimensionality reduction methods listed in Table 2 were applied to the clustered spectral data as shown below.

Cluster Plots:

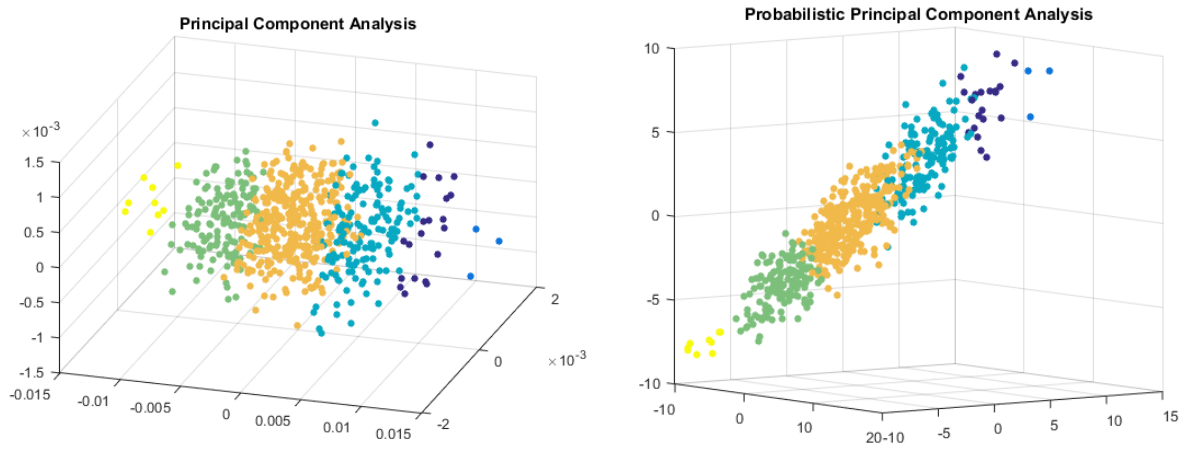

Figure 16: (LEFT) - Principal Component Analysis applied to the clustered Santos Morph spectral data; (Right) – Probabilistic Principal Component Analysis applied to the clustered Santos Morph spectral data

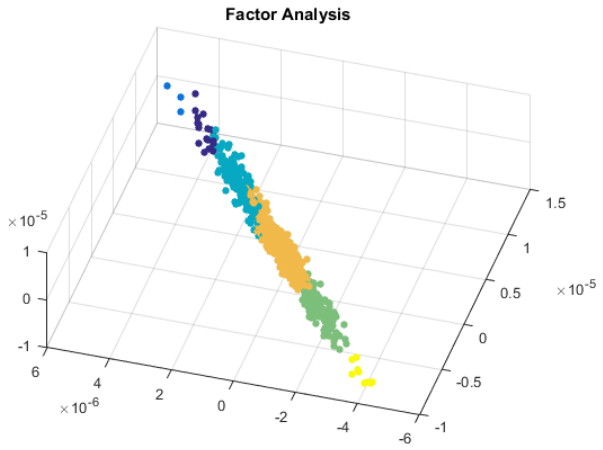

Figure 17: Factor Analysis applied to the clustered Santos Morph spectral data

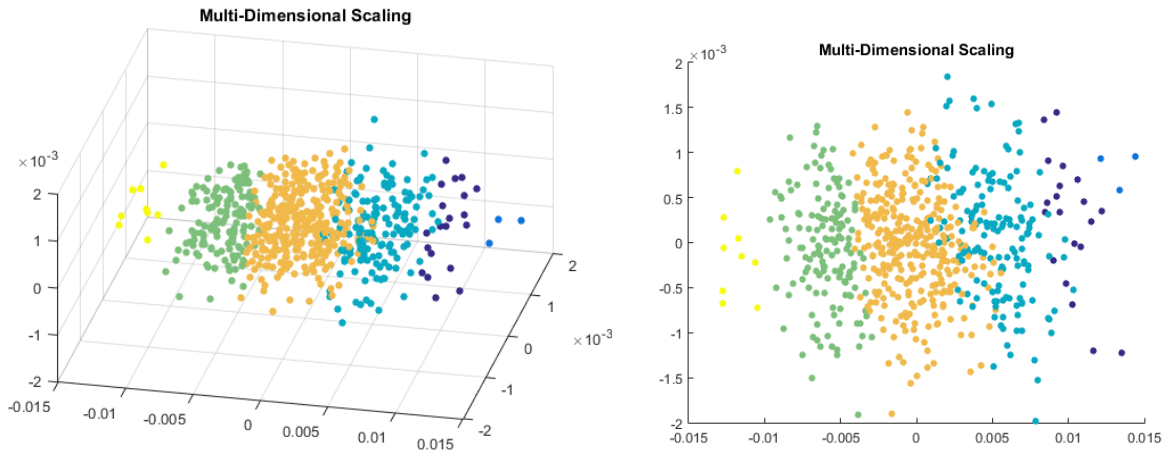

Figure 18: Classical Multi-Dimensional Scaling applied to the clustered Santos Morph spectral data in 3D (Left) and 2D (Right)

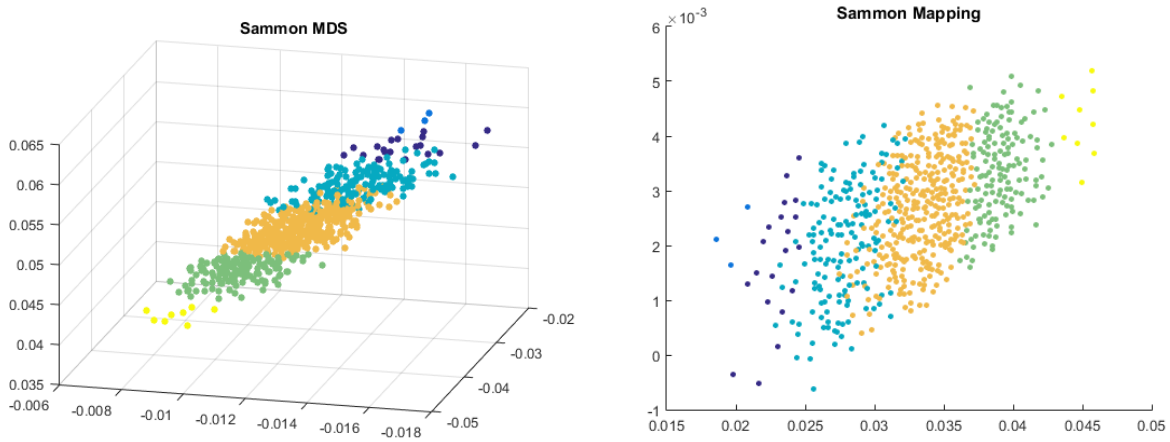

Figure 19: 3D- Sammon Mapping applied to the clustered Santos Morph spectral data in 3D (Left) and 2D (Right)

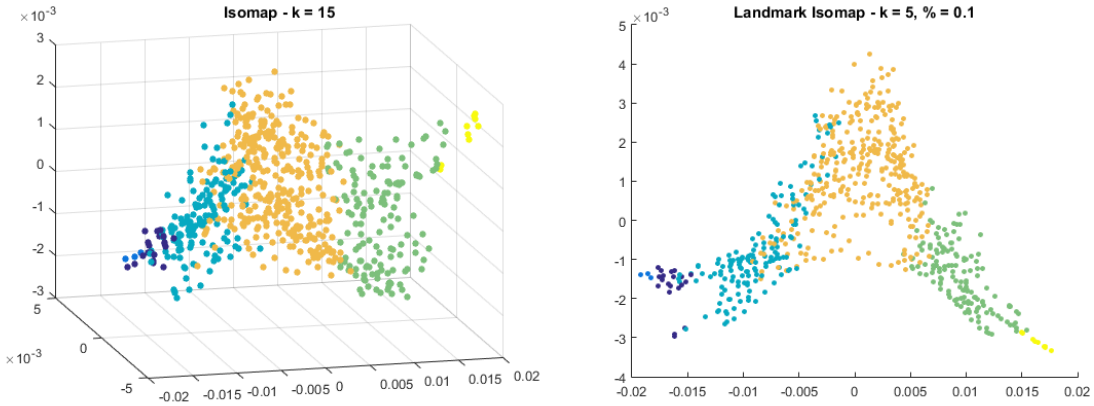

Figure 20: (Left) -3D Isomap applied to the clustered Santos Morph spectral data using k = 15 neighbors; (Right) - 2D Landmark Isomap applied to the Santos Morph spectral data using k = 5 neighbors and 10% landmarks

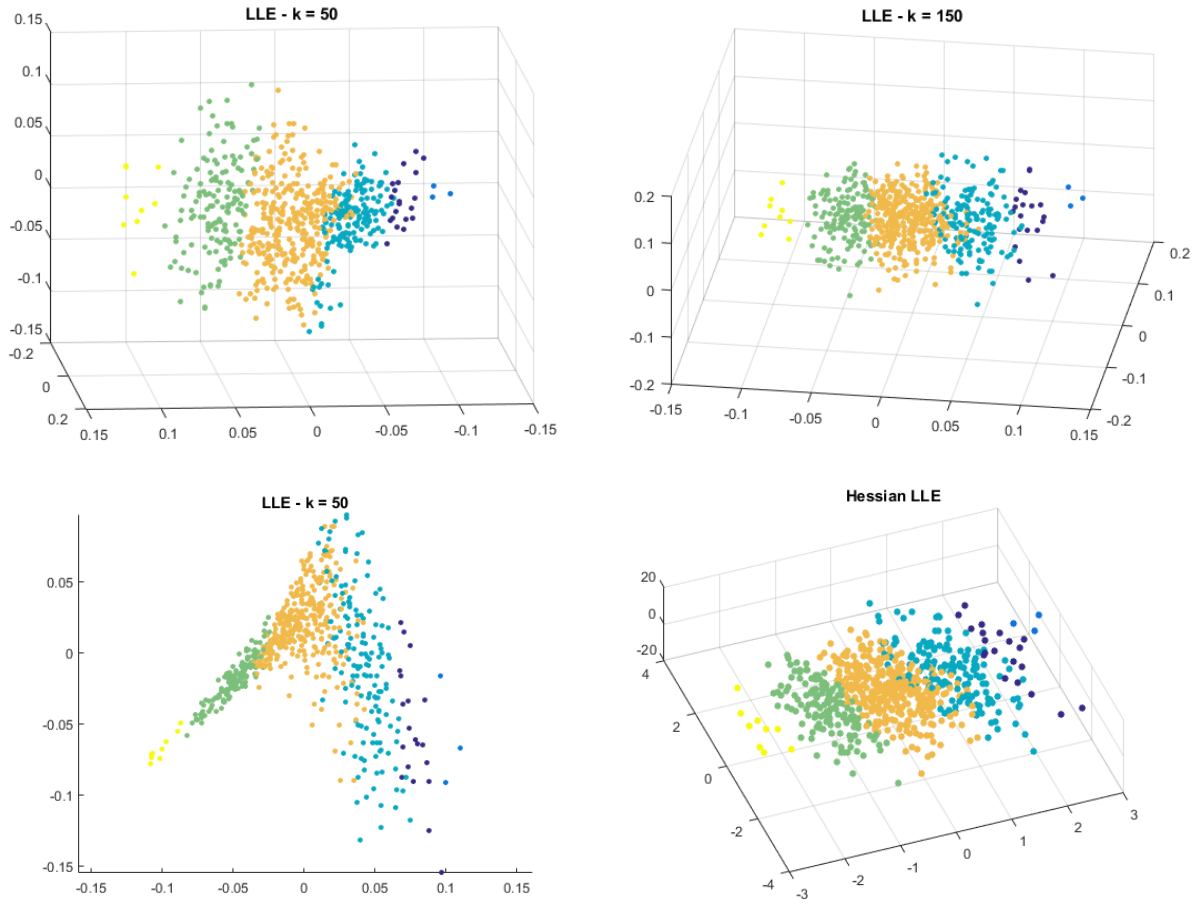

Figure 21: (Top) - Local Linear Embedding applied to the Santos Morph spectral data in 3D using k = 50 neighbors (Left) and k = 150 neighbors (Right); (Bottom) - Local linear Embedding applied to the Santos Morph sepctral data using k =50 neighbors in 2D (Left) and the 3D Hessian LLE formulation (Right)

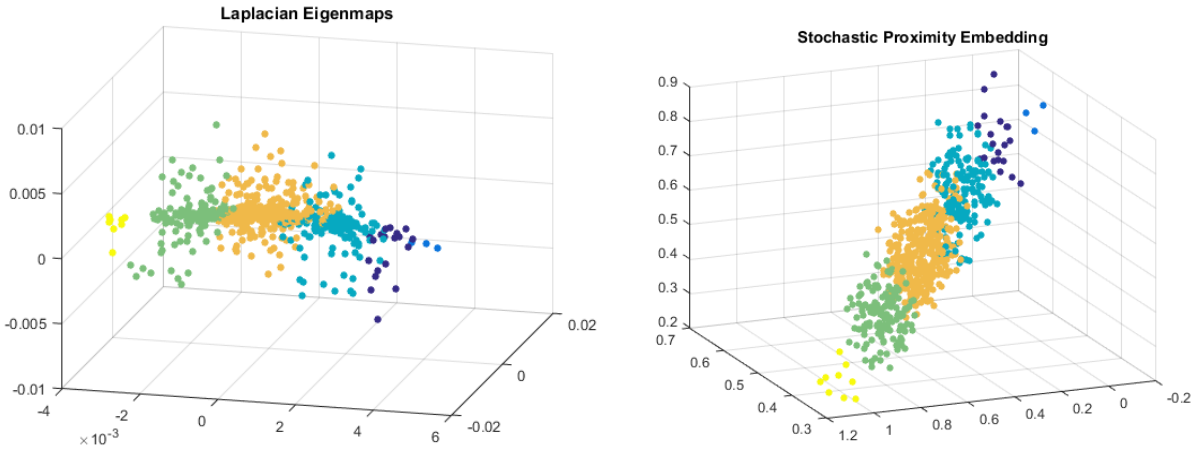

Figure 22: Laplacian Eigenmap (Left) and Stochastic Proximity Embedding (Right) of the Santos Morph spectral data

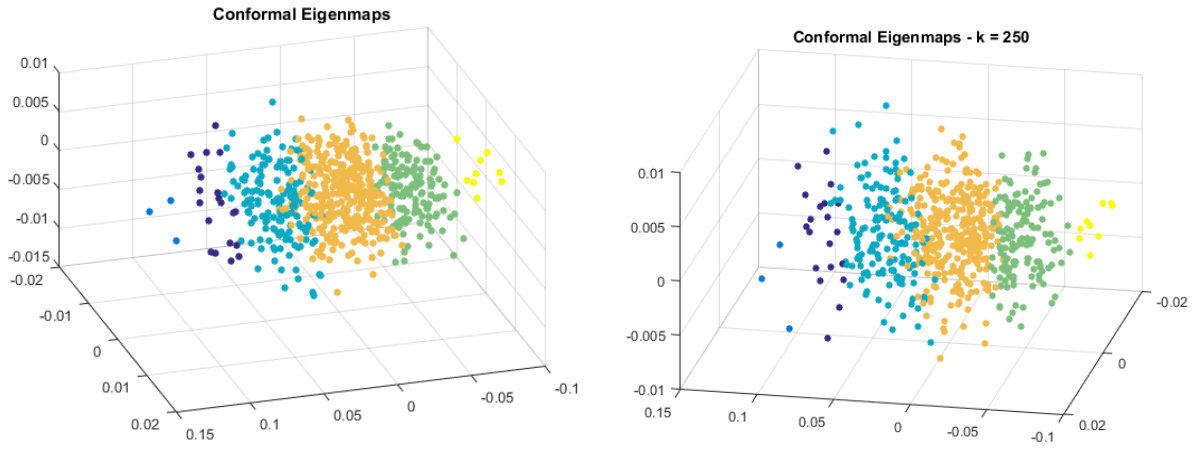

Figure 23: Conformal Eigenmaps (an extension of LLE) applied to the Santos Morph spectral data using k = 150 neighbors (Left) and k = 250 neighbors (Right)

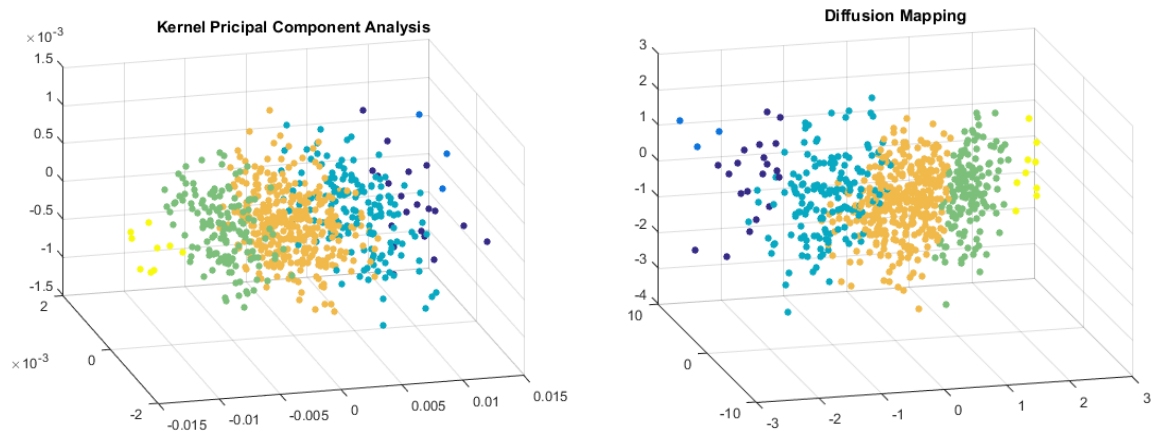

Figure 24: (Left) Kernel Principal Component Analysis and (Right) Diffusion Mapping applied to the Santos Morph spectral data

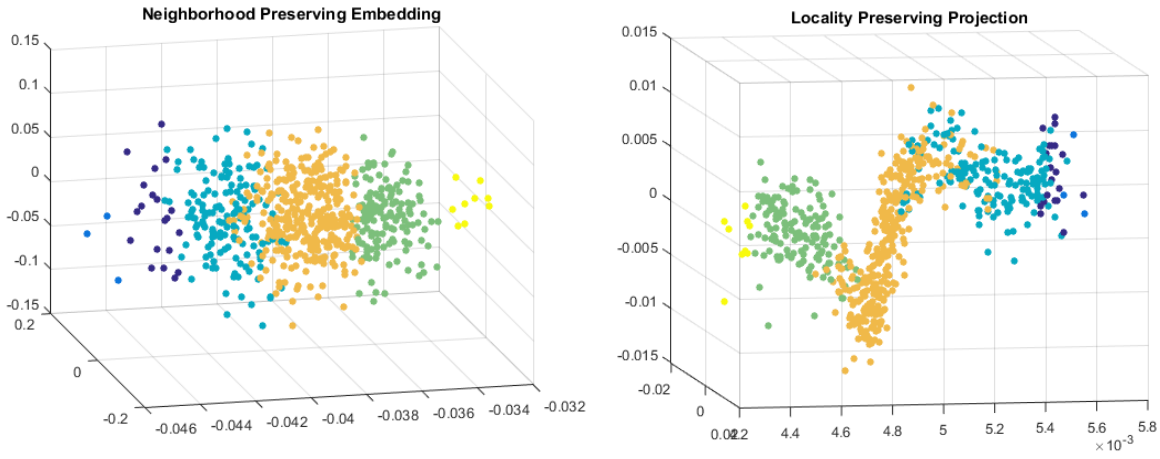

Figure 25: Neighborhood Preserving Embedding (Left) and Locality Preserving Projection (Right) applied to the Santos morph spectral data

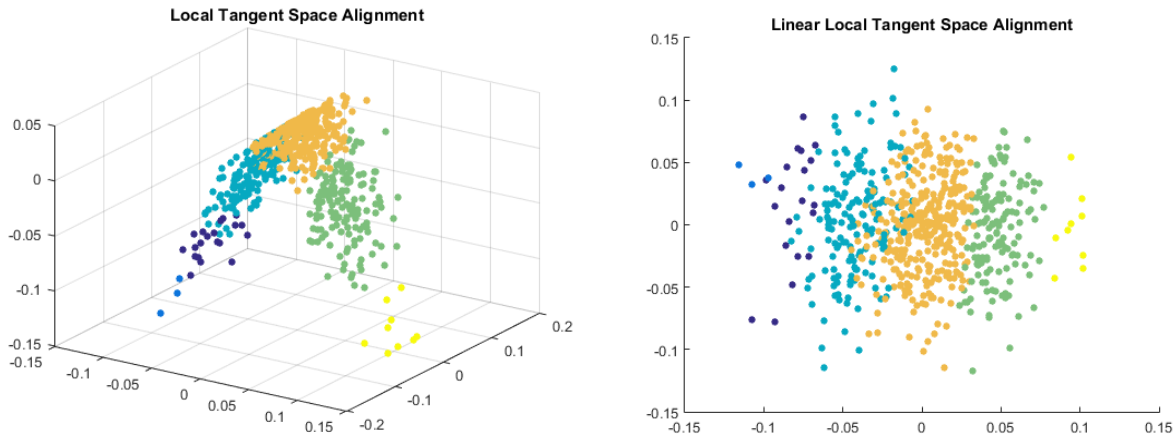

Figure 26: Local Tangent Space Alignment (LTSA) (Left) and Linear LTSA (Right) applied to the Santos Morph spectral data

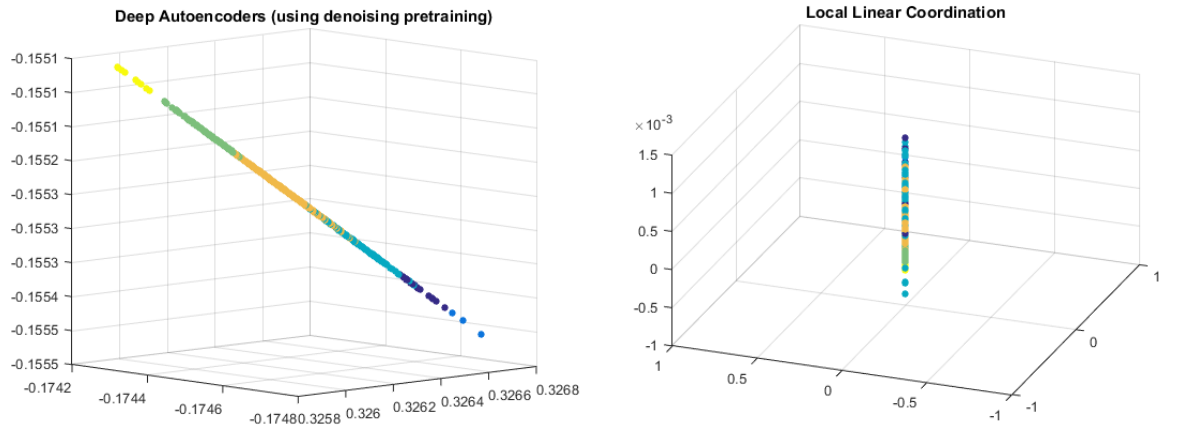

Figure 27: Deep Autoencoders (Left) and Local Linear Coordination (Right) applied to the Santos Morph data, showing the results of an improperly tuned dimensionality reduction method

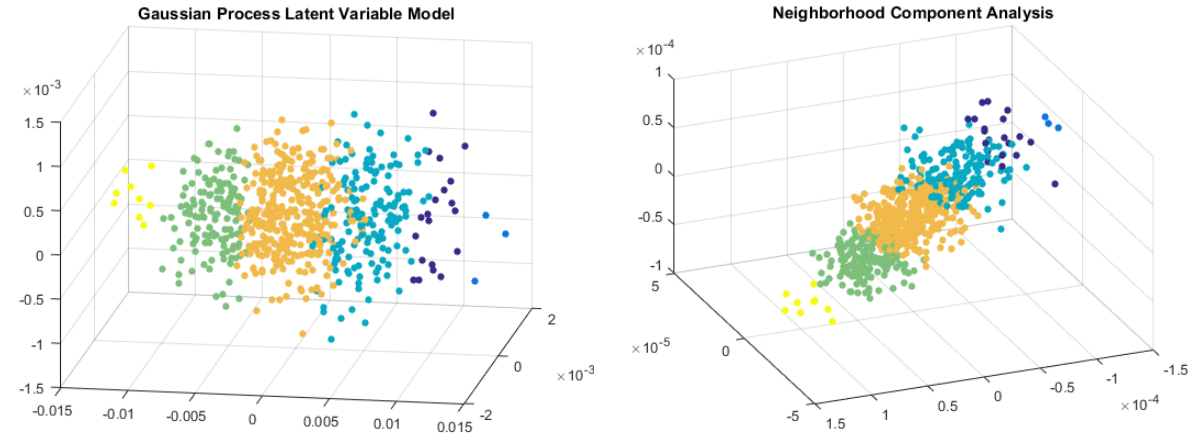

Figure 28: Gaussian Process Latent Variable Model (Left) and Neighborhood Component Analysis (Right) applied to the Santos Morph data

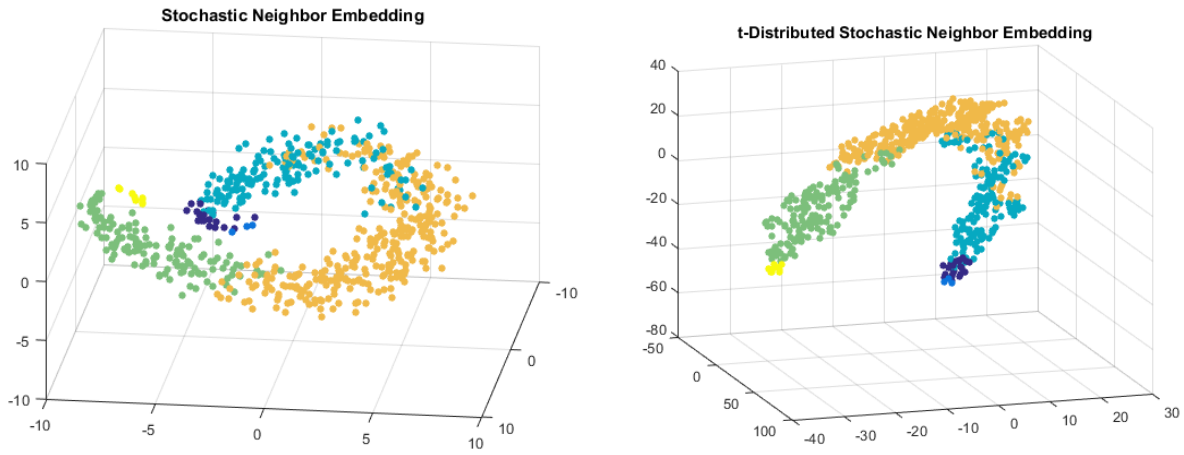

Figure 29: Stochastic Neighbor Embedding (Left) and t-Distributed Stochastic Neighbor Embedding (Right) applied to the Santos Morph data

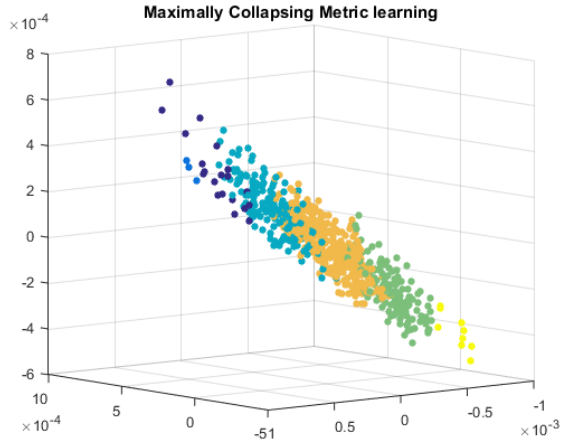

Figure 30: Maximally Collapsing Metric Learning applied to the Santos Morph spectral data

As can be observed from the figures above, there is quite a large amount of variation in the results of the various dimensionality reduction techniques currently available. While many look relatively similar there are inherent differences such as the trend to produce planar results, or in some poorly tuned cases the result is roughly 1D and chaotic (Figure 27). Of the above methods it would appear that the Sammon Mapping (Figure 19), Neighborhood Component Analysis (Figure 28, right), and Stochastic Proximity Embedding (Figure 22, Right) are best suited to the plotting of the human body shape space via their spectral representation.

6.4 - Statistically Representative Models: Initial Results:

The figures in the previous section, while highly variable, provided the insight into the method best suited to visualize the dataset of generated Santos Morph models. As mentioned in the previous section, the Sammon mapping method showed a useful reduction of order that could be used for further analysis of the clustering parameters. As can be observed from the figures in the previous section there is a large amount of disparity between the populations of each cluster, with one of the clusters containing only 3 models. This in mostly due to the mixed gender nature of the dataset, as will be shown later in this section.

While there is some overlap in the larger clusters, this is unavoidable and a result of the dimensionality reduction approximations. These clusters, however, are for a mixed gender dataset. For the purposes of experimentation on the general human body shape a set of representative models were created without any gender distinctions. The formulation of the representative models is rather elementary thanks to the consistent mesh structure throughout all of the morph models. The cluster identifications are first used to identify the models for each cluster, and following that the coordinate information for each vertex is simply averaged across the cluster. As a result, a new model is generated that is representative of its statistical cluster. These models can be found below in Figure 31 and can be seen to cover a wide variety of body sizes and proportions across both genders.

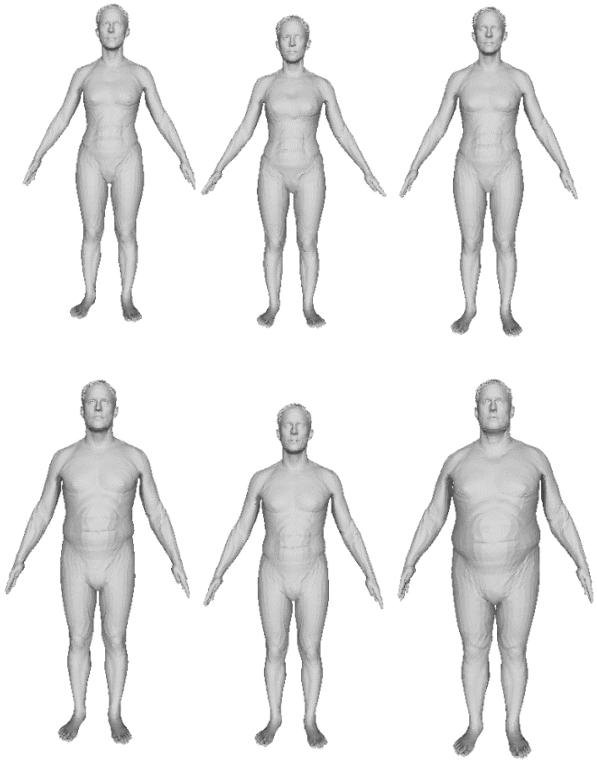

Figure 31: Statistical models generated as averages of the clustered sections of Santos Morphs, in order of their cluster ID.

6.5 – Statistically Representative Models: Gender Specific Results

Clustering and Model Generation:

To generate the most useful statistical models possible it is imperative to separate the male Morphs from the female. This reduction in the variability of body shapes allowed for a finer tuning of the clustering parameters for a more evenly distributed set of cluster populations. By utilizing the Euclidean distances and Ward linkage analysis the data for both the male and female models was clustered into 6 groups. These clusters can be found below, represented via the Sammon Mapping method, in Figure 32.

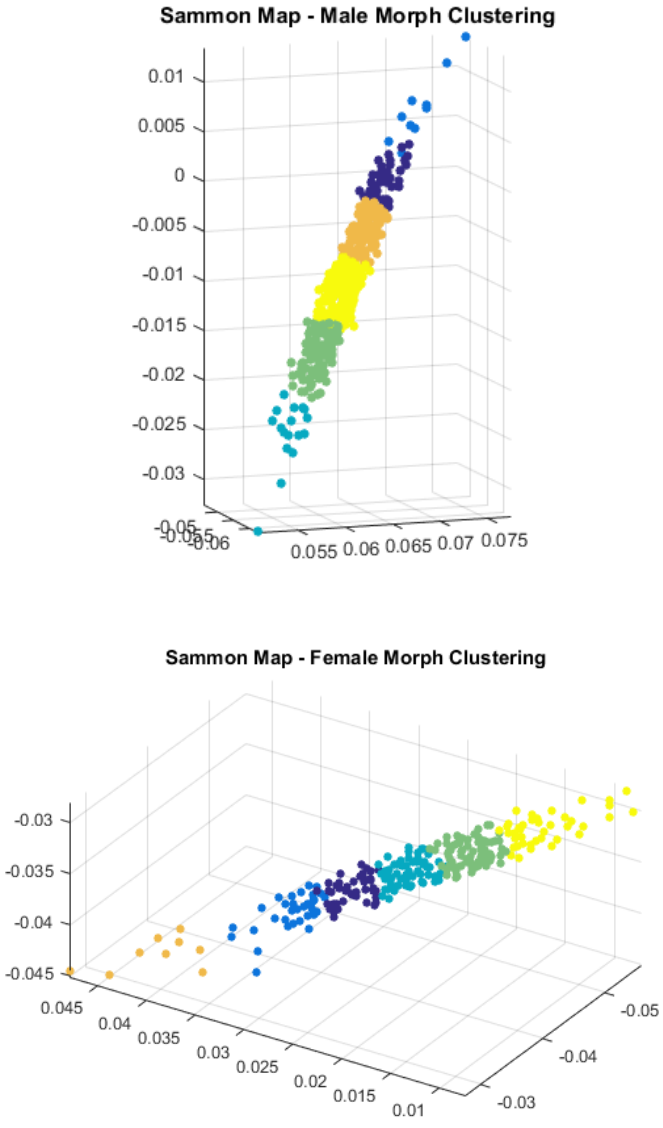

Figure 32: The spectral representations of the Santos Morphs were separated by gender and clustered via an analysis of the Euclidean distances between each model such that each cluster has a sufficient number of models.

The clustering results on the previous page show a much greater level of distinction between the data clusters, as well as the desired reduction in the disparity between cluster populations. This is due to the refinement of each dataset to a single gender, thus reducing the amount of differences between the models being compared. The populations of the resultant clusters can be found in Table 3.

Table 3: Summary of the cluster populations for both the male and female morph datasets after the refinement of the clustering parameters

Cluster ID	*Male Cluster Size:*	*Female Cluster Size:*
1	39	41
2	10	34
3	17	60
4	97	73
5	102	9
6	146	41
Total:	411	258

As can be seen from the table above, while the least populated cluster has only 10 and 9 models for the male and female sets respectively, this is an improvement from the previous distribution. Additionally, the largest cluster has 146 and 73 models for the male and female datasets, respectively. This again makes sense as the male dataset consisted of nearly twice the number of models. While smaller, the female dataset was deemed sufficient to capture the full scope of the population. This difference in the sizes of the male and female scan data is directly from the distribution of male and female data within the CAESAR data. This lends an additional reason to accept the smaller clusters as they are still indicative of a larger group within the general human population.

With the male and female morph data clustered, via the spectral representations of the models, the representative models could be generated for each cluster. Using the process outlined above in section 6.4 the following models (Figure 33 & Figure 34) were generated as the statistically representative models for the general population.

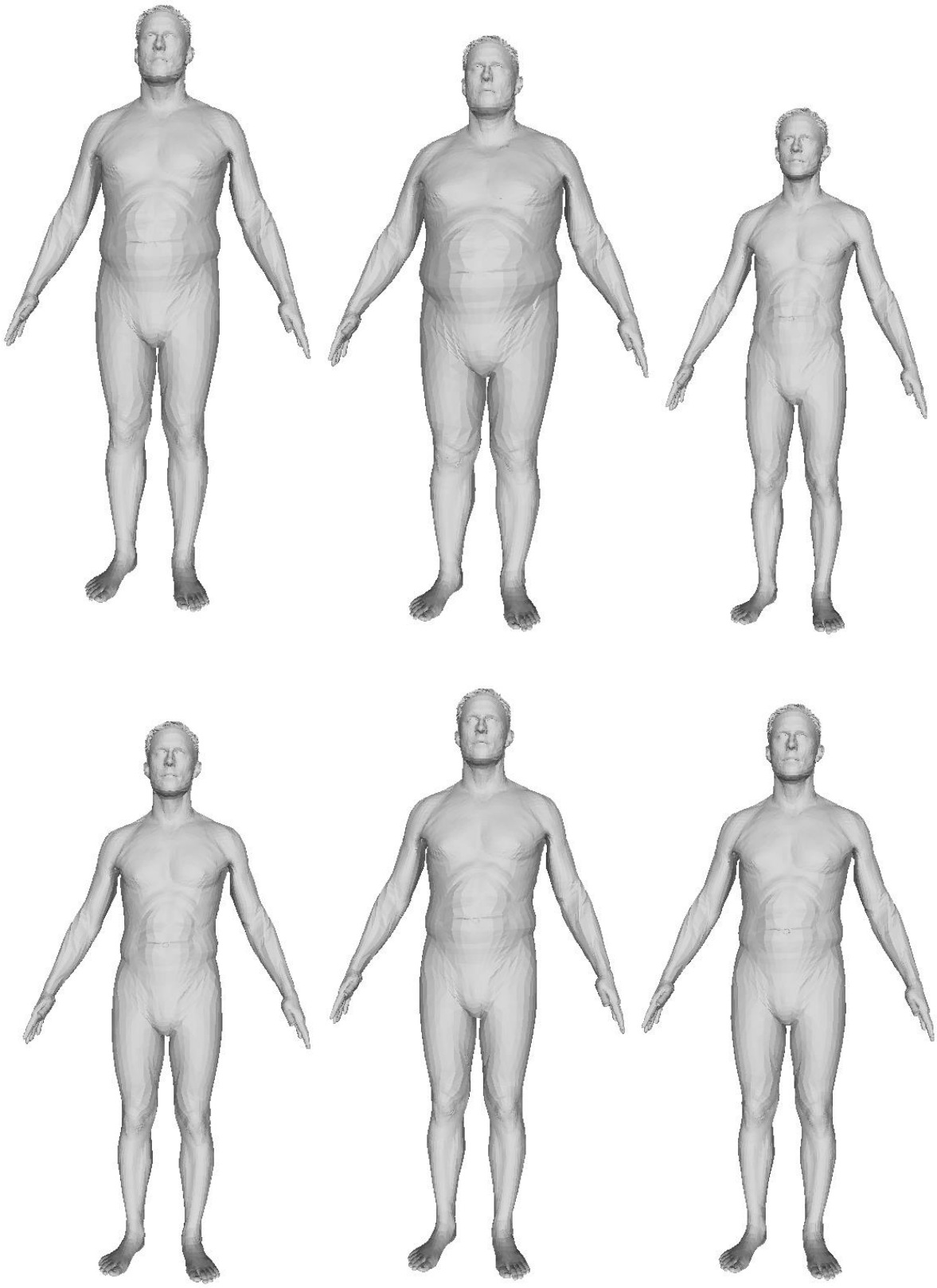

Figure 33: Statistically representative models generated from the clustered spectral data obtained from the male CAESAR dataset and morphed with the SANTOS template model. Clusters are ordered 1-6 from left to right and top to bottom.

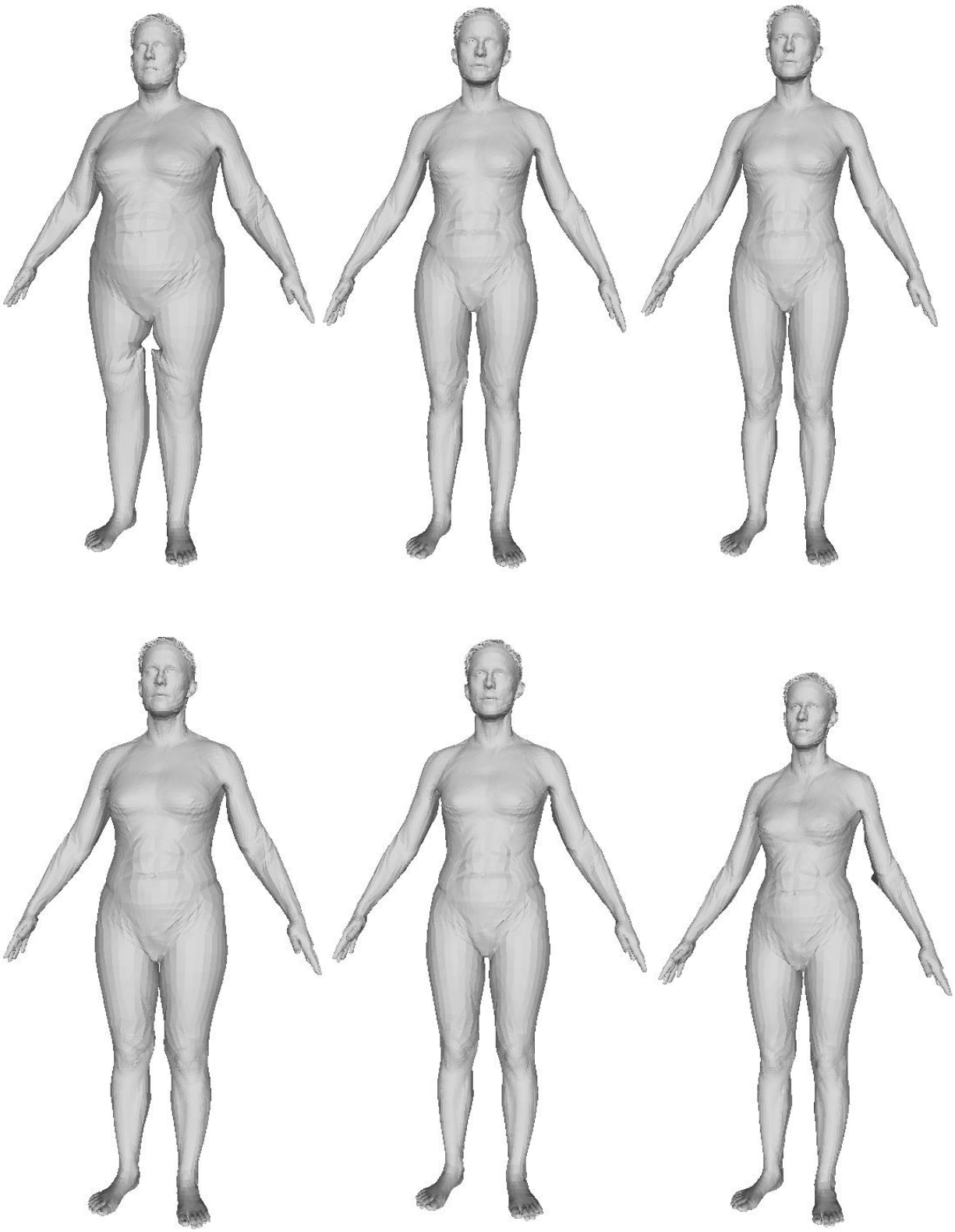

Figure 34: Statistically representative models generated from the clustered spectral data obtained from the female CAESAR dataset and morphed with the SANTOS template model. Clusters are ordered 1-6 from left to right and top to bottom.

Statistical Anthropometry Investigation:

Similar to the generation of the representative models, the anthropometric data corresponding to the models within each cluster could be analyzed as well. To this end, the basic body shape parameters were extracted for each cluster. These parameters consisted of chest girth, neck circumference, sleeve length, and waist circumference. These were determined to be the dominant parameters with regard to the garment industry, with a primary focus on the torso due to the more restrictive sizing system applied by most companies.

Plots were developed to investigate the problematic coupling of these anthropometric sizes in a way that allowed a visualization of the relationships between the parameters, and their association with the clustering. The loose mutual dependence of the parameters can be problematic for designers hoping to narrow the body shape parameter list and this approach allowed for some insight into the relationships between the anthropometric parameters. When comparing the various anthropometric parameters there is a fair amount of overlap between the clusters. This overlap is to be expected however as the clustering is not based on any single parameter but the full shape of the body itself. It is the claim of this research that this formulation of the clustering independent of the raw anthropometric data will result in more accurate grouping of the body shapes. To this end, it can be seen that the organization of the clusters increases greatly when the number of parameters considered is increased, as this better approximates the full body shape that the clusters are based on. However, the clusters remain relatively scattered after the inclusion of the 3rd parameter as this is still an insufficient approximation of the human body shape compared to the spectral representation.

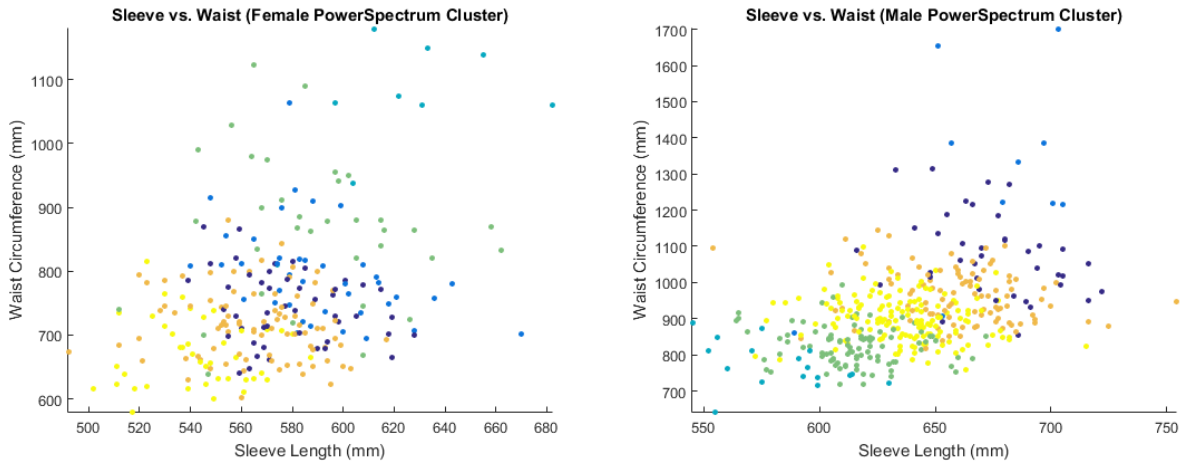

Figure 35: Sleeve Length vs Waist Circumference displaying the relationships between the anthropometric parameters from the CAESAR database for the male and female models used in the clustering, colored to indicate their respective clusters.

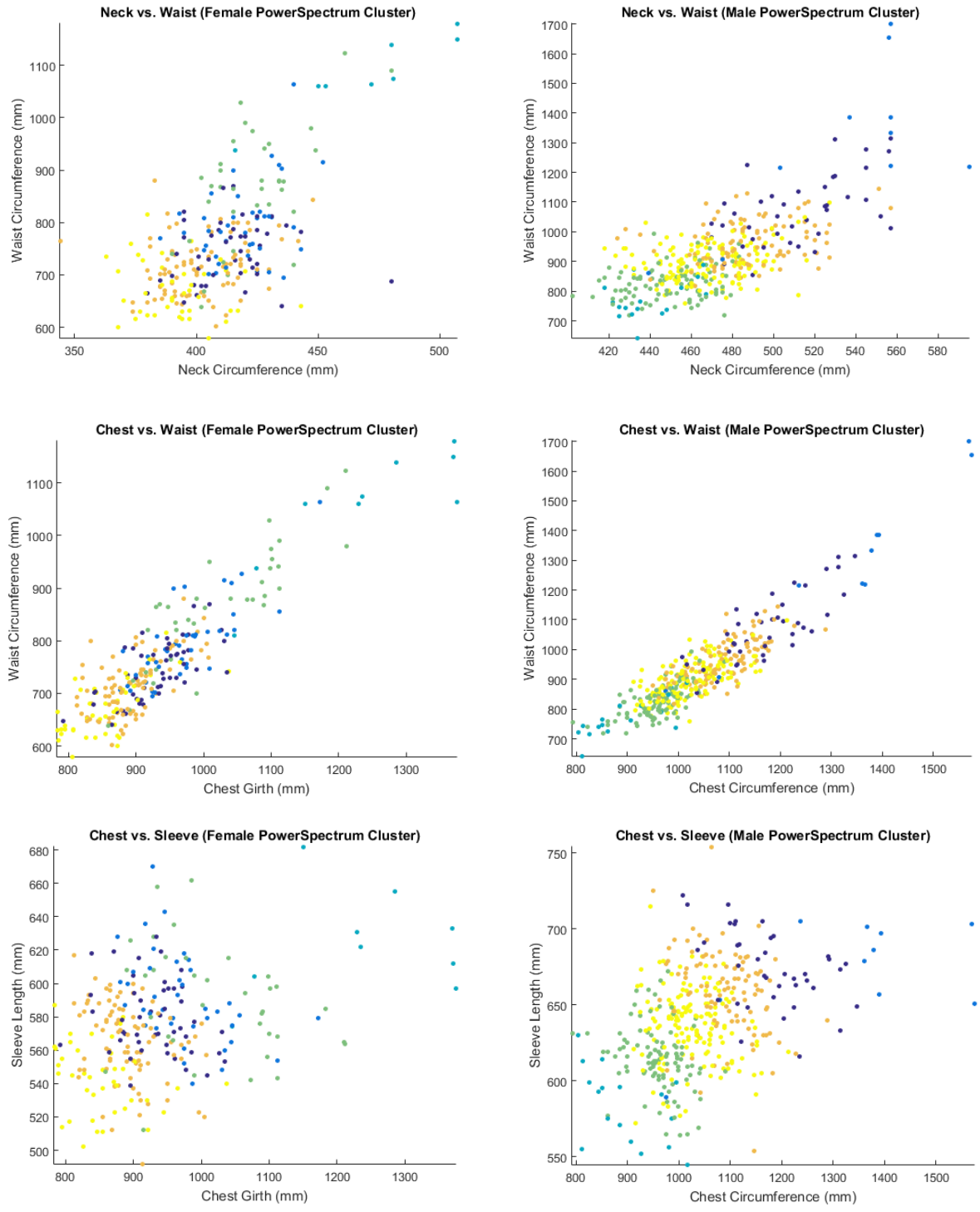

Figure 36: Anthropometric parameter relationship comparisons, plotting the anthropometry data for the morphed and clustered models to investigate the realtionships between the various parameters and their association with the clustering.

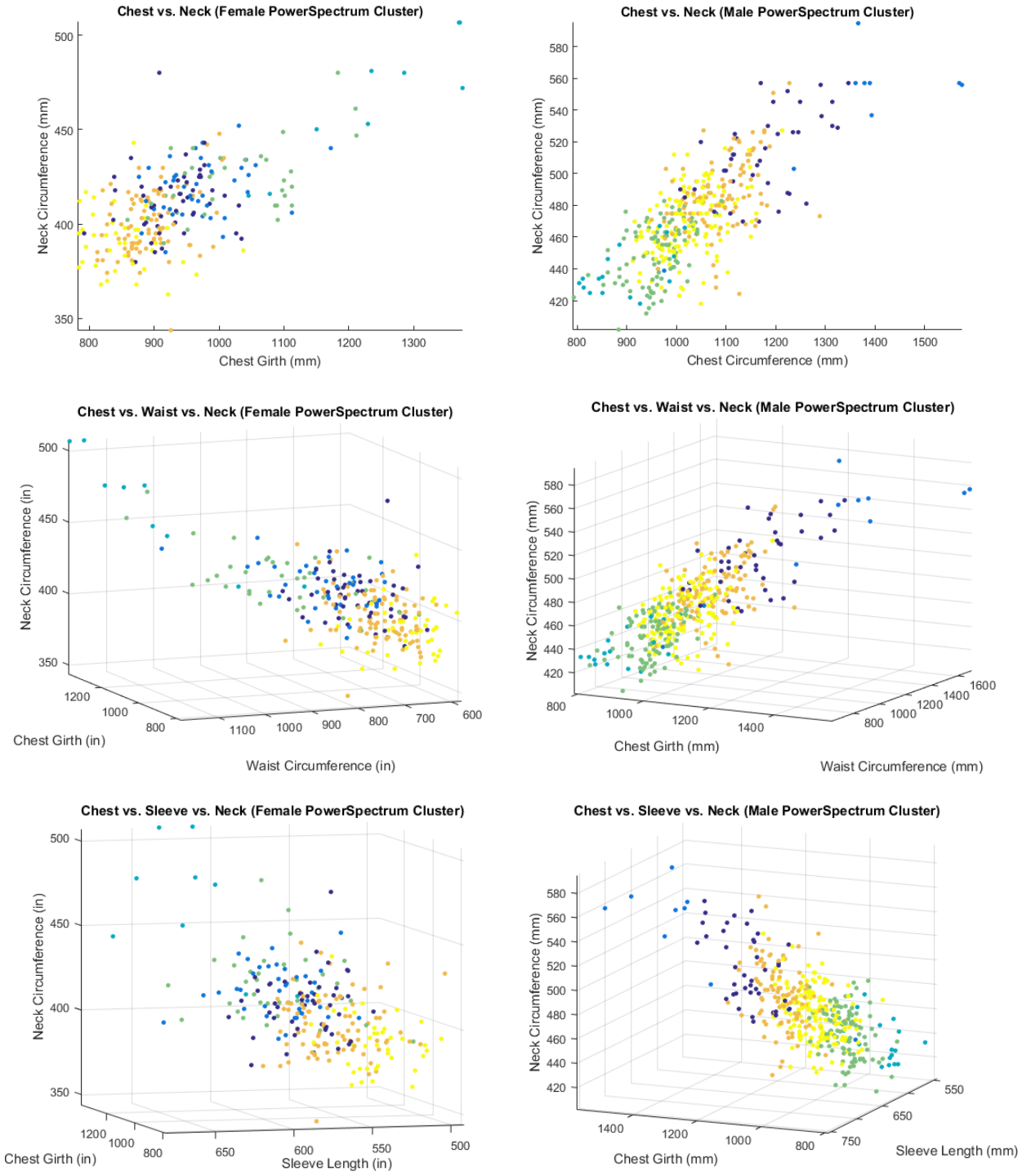

Figure 37: Anthropometric parameter relationship comparisons, plotting the anthropometry data for the morphed and clustered models to investigate the realtionships between the various parameters and their association with the clustering. Additionally, by adding a 3rd parameter it can be seen that the clustering becomes more organized as the parametric approximation of the body shape is improved, but remains relatively scattered.

Accuracy of Anthropometric Clustering in Industry:

In the modern garment industry most upper-body wear comes classified by a single parameter, i.e. small medium large etc. This single sizing parameter was then investigated using the anthropometric values that companies listed within their "sizing charts' in comparison to those represented by the CAESAR dataset. To validate these sizes, and their respective anthropometric lengths, a percentage fit was implemented to identify what percent of the population did not fit into one of the specified sizes. The results ranged from 99.82% to 44.28% of the data falling outside the anthropometric ranges, depending on the brand. While these numbers seem shocking it should be noted that for subsets of the parameters the numbers improve, but when used as a full set they are indicative of a major problem.

Table 4: Anthropometric Sizing chart for Brand "A" used by a garment manufacturer operating in the areas represented by the CAESAR dataset. Calculated at the bottom are the number of people in the entire CAESAR database that fit all of the anthropometric requirements for each size category. The "Size Allowance" was implemented to account for the gaps between the sizes to ensure that each parameter had a continuous inclusion.

Brand "A" Sizing Chart - Inches

	XS	S	M	L	XL	XXL	Size Allowance
Neck (Min)	13	14	15	16	17	18	0.5
Neck (Max)	13.5	14.5	15.5	16.5	17.5	18.5	0.5
Sleeve	32	32.5	34	35	35.5	36	1.5
Chest (Min)	32	34	38	42	46	50	2
Chest (Max)	34	36	40	44	48	52	2
Waist (Min)	28	30	34	38	42	46	2
Waist (Max)	30	32	36	40	44	48	2
# of people fit:	**0**	**0**	**0**	**1**	**0**	**1**	
# of people remaining	**1125**						
% Outliers	**99.82**						

While the results shown in Table 4 regarding "Brand A" are certainly indicative of a problem, the comparison is not entirely reasonable as it requires an individual to fit in the brackets for each anthropometric parameter. To account for people wearing clothes slightly bigger than the recommendation the "Size Allowance" was implemented that was used to widen the size brackets. This was done by dropping the minimum values by a values determined by the maximum gap between the size brackets. In this way the valid range for each parameter was continuous, and yet the results determined only 2 of 1127 people "fitting."

In an attempt to investigate this issue further another brand was examined as shown in Table 5. While the results of the investigation into Brand B are significantly better than that of Brand A, the comparison between the two is not fair due to Brand B listing both less anthropometric parameters and more size categories. That being said, however, Brand B managed to include over half the population with the percentage of outlier body shapes determined to be 44.28%.

Table 5: Anthropometric Sizing chart for Brand "B" used by a garment manufacturer operating in the areas represented by the CAESAR dataset. Calculated at the bottom are the number of people in the entire CAESAR database that fit all of the anthropometric requirements for each size category. The "Size Allowance" was implemented to account for the gaps between the sizes to ensure that each parameter had a continuous inclusion.

Brand "B" Sizing Chart - Inches

	XS	S	M	L	XL	2XL	3XL	4XL	5XL	Size Allowance
Chest (Min)	30	34	38	42	46	50	54	58	62	2
Chest (Max)	32	36	40	44	48	52	56	60	64	2
Waist (Min)	24	28	32	36	40	44	48	52	56	2
Waist (Max)	26	30	34	38	42	46	50	54	58	2
# of people fit:	**1**	**44**	**242**	**243**	**79**	**19**	**7**	**1**	**0**	
# of people Remaining	**499**									
% Outliers	**44.28**									

To compare these size categories to those generated by the spectral clustering analysis a sizing chart was developed for the clusters. This was done by taking the average of each anthropometric parameter across the cluster, and subsequently applying the "Size Allowance" used for each parameter previously to generate a maximum and minimum value for each parameter. While this allowance ensured a continuous range across each variable when applied to the commercial size charts this is not the case with the clustered data groups as they are not linearly separated. However, this formulation does enforce that the allowable range for each parameter is of equal value compared to the commercial charts therefore allowing a legitimate comparison between the groups as they are of equal size with regards to the defining parameters. The size chart for the male data can be found below in Table 6.

Table 6: The ranges for each of the anthropometric parameters used by the commercial size charts, with values determined by taking the average of each parameter across the clusters and subsequently applying the "Size Allowance" determined from the commercial charts to generate the max and min from the averages.

Cluster Sizing Metrics - Inches

	Cluster ID	1	2	3	4	5	6
Chest	**Min**	44.26	50.44	33.21	35.78	40.86	38.34
	Max	48.26	54.44	37.21	39.78	44.86	42.34
Waist	**Min**	40.28	48.72	28.40	30.52	35.90	33.38
	Max	44.28	52.72	32.40	34.52	39.90	37.38
Sleeve	**Min**	25.03	24.96	21.47	22.70	24.45	23.53
	Max	28.03	27.96	24.47	25.70	27.45	26.53
Neck	**Min**	19.66	20.50	16.83	17.22	18.69	17.97
	Max	20.66	21.50	17.83	18.22	19.69	18.97

With the size chart developed for the male clustered data a comparison was done with the effectiveness of the commercial brand's size categories. By applying the same requirements, with regards to the anthropometric parameters involved, the clustered groups show significant improvements in the percentages of people fitting all of the categories. The Brand A comparison shows a 16.95% improvement, and similarly the Brand B comparison shows a 15% improvement.

Table 7: Comparison of the results for the spectral clustering groups as formulated from the Brand A and Brand B parameters. Each of the two comparisons accounts for the same variables listed in the respective sizing charts but with the values determined by taking the average of the parameter across the cluster and applying the same "Size Allowance" in such a way that, while not continuous, the span of the parameter is the same for each cluster as it is in the Brand Size allotments.

Brand A comparison	***# of "1"***	***# of "2"***	***# of "3"***	***# of "4"***	***# of "5"***	***# of "6"***
	2	**0**	**16**	**53**	**34**	**88**
# of people fit	**193**					
# of people remaining	**934**					
% unmatched	**82.87**					

Brand B comparison	***# of "1"***	***# of "2"***	***# of "3"***	***# of "4"***	***# of "5"***	***# of "6"***
	12	**0**	**131**	**269**	**113**	**272**
# of people fit	**797**					
# of people remaining	**330**					
% unmatched	**29.28**					

While the results of the spectral clustering are much better than those of the commercial size charts a fair amount of people remain outliers when required to fit within a single category across the full range of anthropometric parameters. To investigate this figures were developed, similar to Figure 35 - Figure 37, to compare the relationships between the anthropometric parameters. However, in this examination the spectral clusters are represented by the ranges defined in the size chart shown above in Table 6 as opposed to the color identification on each point as the data points are from the CAESAR anthropometric data set and not necessarily associated with a cluster.

To determine the reason for the poor fitting results of Brand A the parameters were plotted in a way that identified the Neck circumference as the predominant source of the errors, as shown in Figure 38.

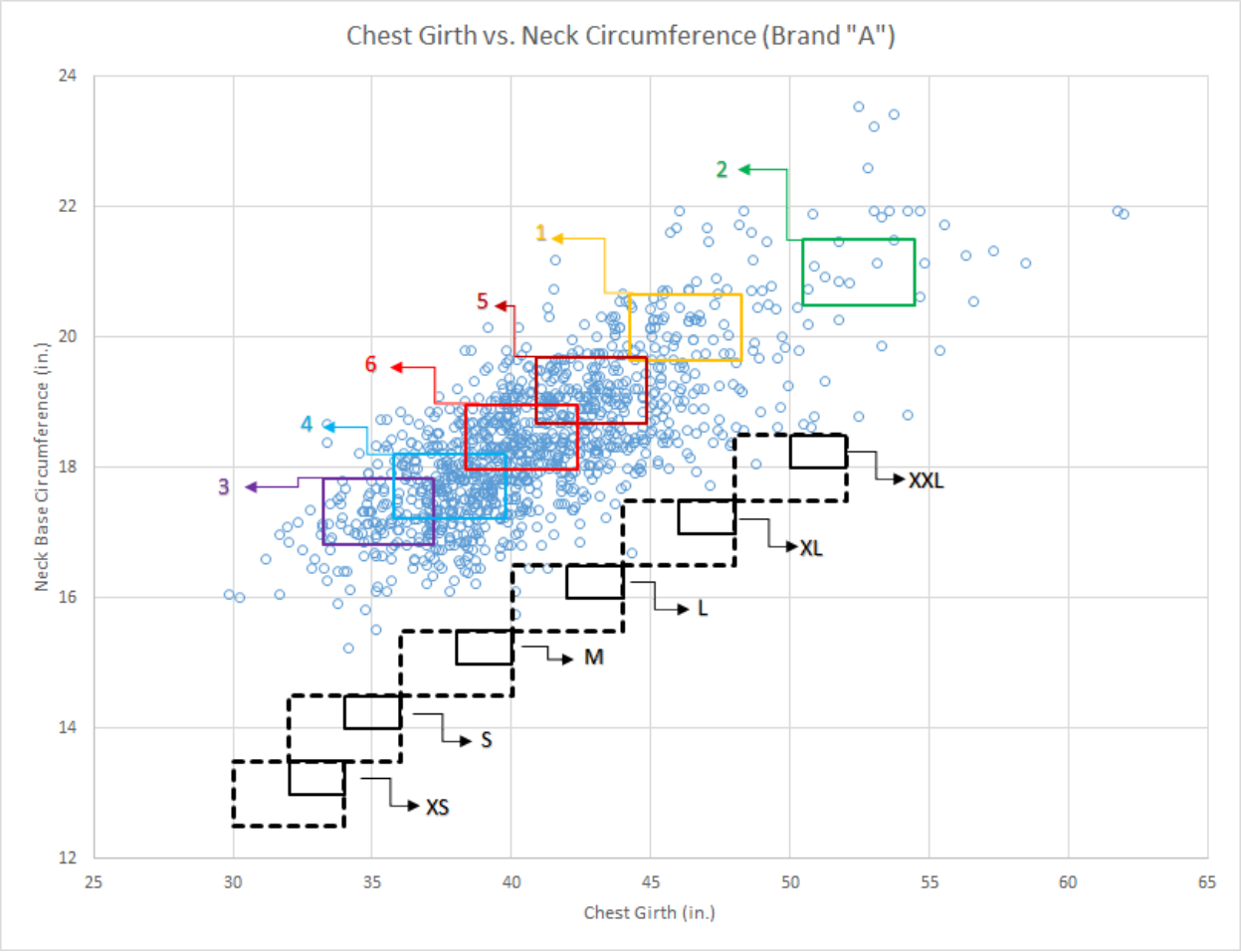

Figure 38: Comparison of the Neck circumference and Chest girth ranges for both the spectral cluster groups (Colored) and the sizing requirements of Brand A (Black) with the solid line showing the true size bracket and the dashed line indicating the increased range due to the application of the size allowance.

While Figure 38 alone does not specify the neck values as the error source, when comparing the chest and waist values (Figure 39) the association with the data is shown to be much improved thereby identifying the neck as the problematic parameter regarding the parameters used by Brand A.

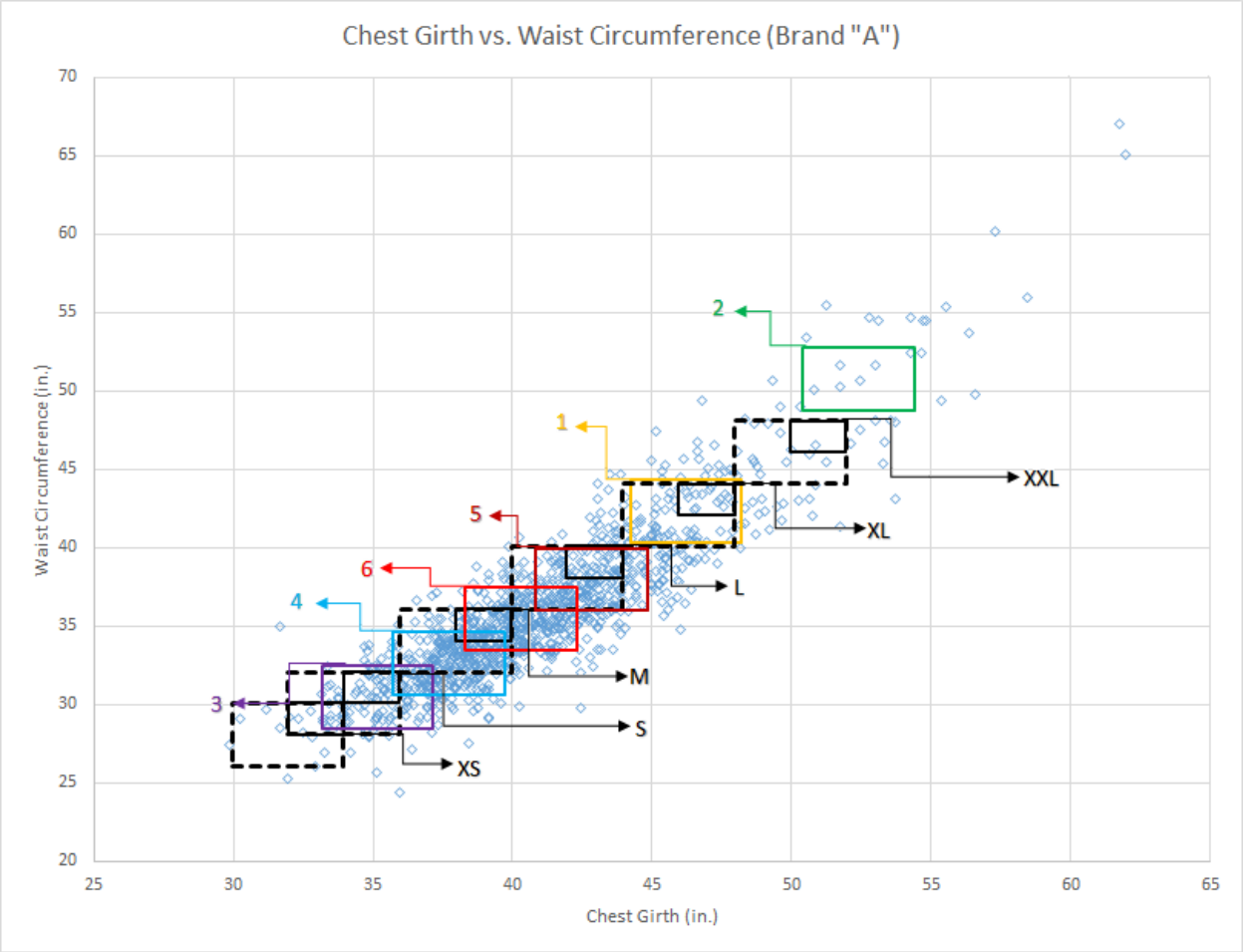

Figure 39: Comparison of the Neck circumference and Chest girth ranges for both the spectral cluster groups (Colored) and the sizing requirements of Brand A (Black) with the solid line showing the true size bracket and the dashed line indicating the increased range due to the application of the size allowance.

It is clearly evident from the figures above that the spectral clustering formulation results in an improved grouping of the human body sizes and shapes. While the spectral clusters show a much greater association with the actual anthropometric data they also show a grouping that is more indicative of the true distribution of the human body shapes as they are concentrated in the same areas of the densest levels of human body shapes. The seemingly Gaussian distribution along each anthropometric parameter leads to a concentration of similar body shapes that is better accounted for by the spectral clusters as opposed to linearly offset size categories. Additionally, this lack of linear rigidity allows the spectral clusters to better approximate the true behavior of the parameters which can be parabolic to a minor degree at the extremes of the ranges.

Similar to the figures above, the anthropometric data was plotted for the parameters specified by Brand B, as shown in Figure 40. Once again the spectral cluster groups show a better association with the data than those of the commercial size brackets for the same reasons discussed previously.

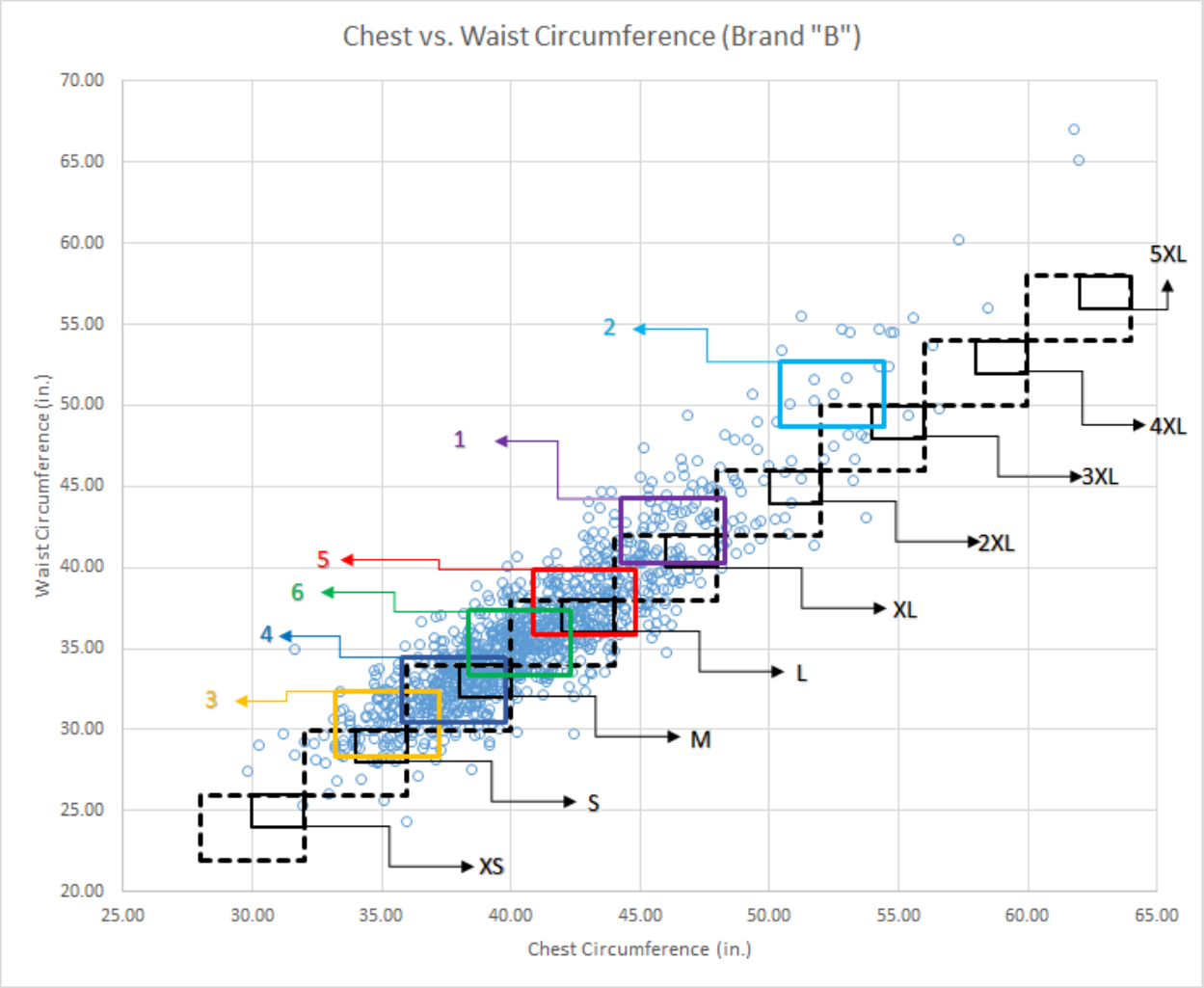

Figure 40: The Chest girth and Waist circumference data for the CAESAR dataset is plotted with the bounds for the sizing categories specified by Brand B as well as the bounds generated from the spectral clustering groups for a comparison of their association with the anthropometric data.

While both Brand A and Brand B showed relatively accurate agreement with the anthropometric data, regarding the chest and waist parameters, the spectral clustering groups provide a better fit to the data. This is especially true regarding the extremes of these parameters, as well as capturing the greater density of people in the more average range.

This anthropometric accuracy analysis serves to validate the clusters relation to the derivative data. This, in turn, validates the representative models whose body shapes would place them at the center of their respective cluster groups.

Chapter 7: Discussion & Conclusions

The high levels of reality achieved by modern digital human models has established human-centered design as an essential method for product development. These modern digital humans have additionally enabled many researchers to develop simulation engines capable of highly detailed analysis regarding the biometrics and kinetics / dynamics of the model. However, while the capabilities of the simulation engines such as SantosHuman have continued to progress, they are hindered by a fundamental limitation inherent to the digital human models used. A lack of diversity in the models compatible with the simulation engine presents a significant limitation in the applications available. This lack of diversity is due to the intricate manner in which the model is analyzed by the simulation engine as it often requires the implementation of a musculoskeletal system in addition to the mass / inertial data for the human model. As a result, a significant amount of pre-processing is required for any human model before it can be used in the simulation that requires high levels of expertise and time.

The process outlined in this research provides an efficient solution to this limitation that greatly increases the scope of these simulation engines by providing a method to generate compatible human models with two major advantages beyond their compatibility. Firstly, the method allows for a "free" exploration of the human body shape within the human body shape space. Second, a set of statistically representative models was obtained that are not only more anthropometrically accurate than traditional formulations but also more efficiently obtained. These representative models then enable a more efficient human-centered design process as the accuracy of the digital model directly improves the analysis in the design stage of product development.

These advantages were obtained by utilizing recent advancements in multiple fields, primarily big-data analysis and digital modeling methods. A single human model (Santos) was expanded to a mutually compatible set of models by taking advantage of the consistent mesh structure generated by template-based modeling. This enrichment of the Santos shape space provided the first solution to the digital human simulation diversity limitation by populating the so-called shape manifold.

As for the generation of the statistically representative models, the process outlined in this research presents a method that is both more anthropometrically accurate and computationally efficient than traditional methods by utilizing the Metric Dependent Spectrum as a shape descriptor. While spectral shape representation offers numerous benefits in theory, the discretization method of the Shape Operator required validation. By applying the spectral shape representation process to a set of isometric models, and comparing the results to a set of characteristics required for its implementation, it was shown that not only is the Metric Dependent Spectrum a valid operator but that it is in fact an improved version of the traditional

Laplace-Beltrami Operator formulations. This spectral shape descriptor was then used to reduce the dimensionality of the Santos Morph dataset, allowing for an efficient analysis of the models, as well as a visualization of the shape manifold. This reduced dimensionality of the models enabled the application of a clustering algorithm to identify the statistical segments of the population that would not be possible otherwise, as explained in Chapter 6. Using this statistical cluster information, the representative models could be obtained that presents the second solution to the dominant limitation of human simulation engines. The scope of the applications for these representative models extends beyond these research-based simulation projects however, as they present a better anthropometric representation of the human population that benefits the commercial sector from garment design to digital human modeling companies such as CadHuman *etc*.

For validation of the statistical models, however, attention was focused on the garment industry due to its dependence on anthropometric accuracy. By examining the anthropometric data used by commercial garment manufacturers, and comparing it with the CAESAR anthropometric data, a large amount of disparity was found. When this process was repeated with the spectral cluster data that defined the representative models the spectral clustered data was shown to have a much better level of agreement with the CAESAR data. The spectral clusters were shown to provide a minimum improvement of a 15% increase in the amount of people that fit into the defined categories when compared to multiple commercial manufacturers. These spectral clusters then provide the guidelines to redesign the sizing groups for garment production that would more efficiently encapsulate the scope of human body shapes.

References:

[Abdel-Malek2006] Abdel-Malek, K., Arora, J., Yang, J., Marler, T., Beck, S., Swan, S., Frey-law, L., Mathai, A., Rahmatalla, S., and Patrick, A. "*Santos: A Physics-Based Digital Human Simulation Environment."* Paper presented at the 50th Annual Meeting of the Human Factors and Ergonomics Society, San Francisco, CA, 2006.

[Abdel-Malek 2007] Abdel-Malek, K., Yang, J., Kim, J. K., Marler, T., Beck, S., Swan, C., Frey-Law, Mathai, A., Murphy, C., Rahmatalla, S., and Arora, J. "*Development of the Virtual-Human Santos*," in Digital Human Modeling – First International Conference on Digital Human Modeling, Proceedings, July, Bejing, China, Lecture Notes in Computer Science, 4561, Springer-Verlag, Berlin, 490-499, 2007.

[Allen2003] Brett Allen, Brian Curless, Zoran Popović, "*The space of human body shapes: reconstruction and parameterization from range scans*," Proceedings of the 30th annual conference on Computer graphics and interactive techniques (SIGGRAPH 2003), pp. 587-594, 2003.

[Allen2006] Brett Allen, Brian Curless, Zoran Popović, and Aaron Hertzmann, "*Learning a correlated model of identity and pose-dependent body shape variation for real-time synthesis*," Proceedings of the 2006 ACM SIGGRAPH/Eurographics symposium on Computer animation, pp. 147-156, 2006.

[Anguelov2005] Dragomir Anguelov, Praveen Srinivasan, Daphne Koller, Sebastian Thrun, Jim Rodgers, and James Davis, "*Scape: shape completion and animation of people*," ACM Transactions on Graphics (TOG), Vol. 24, No. 3, pp. 408-416, 2005.

[Azouz2006] Zouhour Ben Azouz, Marc Rioux, Chang Shu, and Richard Lepage, "*Characterizing human shape variation using 3D anthropometric data*," The Visual Computer, Vol. 22, No. 5, pp. 302-314, 2006.

[Baek2012] Seung-Yeob Baek and Kunwoo Lee, "*Parametric human body shape modeling framework for human-centered product design*," Computer-Aided Design, Vol. 44, No. 1, pp. 56-67, 2012.

[Baek2013] Seung-Yeob Baek, "*Nonlinear Analysis of the Space of Human Body Shapes and Its Application to Parametric Human Modeling System*," Ph.D. Dissertation, Seoul National University, Korea, 2013.

[Baek2016] Seung-Yeob Baek, Samuel S. Mate, Tsz-Ho Kwok, Charlie C. L. Wang, Kunwoo Lee, "*Human Body Shape Modeling Methods for Human-Centered CAD Systems: A survey*", submitted to Computer Aided Design, Elsevier journal, 2016.

[Blanz1999] Volker Blanz, and Thomas Vetter. "*A morphable model for the synthesis of 3D faces*," Proceedings of the 26th annual conference on Computer graphics and interactive techniques (SIGGRAPH '99), pp. 187-194, 1999.

[Bronstein2010] Michael M Bronstein and Iasonas Kokkinos. "*Scale-invariant heat kernel signatures for non-rigid shape recognition*." In Proceedings of IEEE Conference on Computer Vision and Pattern Recognition (CVPR 2010), pages 1704–1711, 2010.

[CadHuman] http://www.cadhuman.com/

[Chu2010] C. H. Chu, Y. T. Tsai, C. C. L. Wang and T. H. Kwok, "*Exemplar-Based Statistical Model for Semantic Parametric Design of Human Body*", Computers in Industry, Volume 61, Issue 6, Pages 541-549, 2010.

[Dubrovina2010] Anastasia Dubrovina and Ron Kimmel. "*Matching shapes by eigendecomposition of the laplace-beltrami operator*." In Proceedings of the International Symposium on 3D Data Processing, Visualization and Transmission (3DPVT), volume 2, 2010.

[Fang2011] Yi Fang, Mengtian Sun, Minhyong Kim, and Karthik Ramani. "*Heat-mapping: A robust approach toward perceptually consistent mesh segmentation*." In Proceedings of IEEE Conference on Computer Vision and Pattern Recognition (CVPR 2011), pages 2145–2152, 2011.

[H-Anim] www.hanim.org

[Hu2012] Jingwen Hu, Kathleen D. Klinich, Matthew P. Reed, Michael Kokkolaras, Jonathan D. Rupp. "*Development and validation of a modified Hybrid-III six-year-old dummy model for simulating submarining in motor-vehicle crashes.*" Journal of Medical Engineering and Physics, Volume 34, Pages 541-551, 2012.

[Kac1966] Mark Kac. "*Can one hear the shape of a drum?*" The American Mathematical monthly, 73(4):1–23, 1966.

[Levy2010] Bruno Levy and Hao Richard Zhang. "*Spectral mesh processing*". In ACM SIGGRAPH 2010 Courses, page 8, 2010.

[Marler2008] Marler, T., Arora, J., Beck, S., Lu, J., Mathai, A., Patrick, A., Swan, C, "*Computational Approaches in DHM,*" in Handbook of Digital Human Modeling for Human Factors and Ergonomics, Vincent G. Duffy, Ed., Taylor and Francis Press, London, England, 2008

[Mateus2008] Diana Mateus, Radu Horaud, David Knossow, Fabio Cuzzolin, and Edmond Boyer. "*Articulated shape matching using laplacian eigenfunctions and unsupervised point registration*." In Proceedings of IEEE Conference on Computer Vision and Pattern Recognition, 2008 (CVPR 2008), pages 1–8, 2008.

[Meyer2002] Mark Meyer, Mathieu Desbrun, Peter Schroder, Alan H Barr, et al. "*Discrete differential-geometry operators for triangulated 2-manifolds.*" Visualization and mathematics, 3(2):52–58, 2002.

[Niethammer2007] Marc Niethammer, Martin Reuter, Franz-Erich Wolter, Sylvain Bouix, Niklas Peinecke, Min-Seong Koo, and Martha E Shenton. "*Global medical shape analysis using the laplace-beltrami spectrum*." In Proceedings of Medical Image Computing and Computer-Assisted Intervention–MICCAI 2007, pages 850– 857, 2007.

[Ovsjanikov2009] Maks Ovsjanikov, Alexander M Bronstein, Michael M Bronstein, and Leonidas J Guibas. "*Shape google: a computer vision approach to isometry invariant shape retrieval*." In Proceedings of IEEE 12th International Conference on Computer Vision Workshops (ICCV Workshops 2009), pages 320–327, 2009.

[Park2006] Sang Il Park, and Jessica K. Hodgins, "*Capturing and animating skin deformation in human motion*," ACM Transactions on Graphics (TOG), Vol. 25, No. 3, pp. 881-889, 2006.

[Reuter2005] Martin Reuter, Franz-Erich Wolter, and Niklas Peinecke. "*Laplace-spectra as fingerprints for shape matching.*" In Proceedings of the 2005 ACM symposium on Solid and physical modeling, pages 101–106, 2005.

[Reuter2006] Martin Reuter, Franz-Erich Wolter, and Niklas Peinecke. "*Laplace–beltrami spectra as 'shape-dna' of surfaces and solids*." Computer-Aided Design, 38(4): 342–366, 2006.

[Reuter2009a] Martin Reuter, Silvia Biasotti, Daniela Giorgi, Giuseppe Patane, and Michela Spagnuolo. "*Discrete laplace–beltrami operators for shape analysis and segmentation.*" Computers & Graphics, 33(3):381–390, 2009a.

[Reuter2009b] Martin Reuter, Franz-Erich Wolter, Martha Shenton, and Marc Niethammer. "*Laplace–beltrami eigenvalues and topological features of eigenfunctions for statistical shape analysis*." Computer-Aided Design, 41(10):739–755, 2009b.

[Santos] Santos Human http://www.santoshumaninc.com/

[Seo2003] Hyewon Seo, Nadia Magnenat-Thalmann, "*An automatic modeling of human bodies from sizing parameters,*" Proceedings of the 2003 Symposium on Interactive 3D Graphics, pp. 19-26, 2003.

[Seo2004] Hyewon Seo, Nadia Magnenat-Thalmann, "*An Example-Based Approach to Human Body Manipulation,*" Graphical Models, Vol. 66, No. 1, pp. 1-23, 2004.

[Shi2009] Yonggang Shi, Jonathan H Morra, Paul M Thompson, and Arthur W Toga. "*Inverse-consistent surface mapping with laplace-beltrami eigen-features.*" In Proceedings of the 21st International Conference on Information Processing in Medical Imaging (IPMI '09), pages 467–478, 2009.

[Wang2005] Charlie C. L. Wang, "*Parameterization and parametric design of mannequins*," Computer-Aided Design, Vol. 37, No. 1, pp. 83-98, 2005.

[Xi2007] Pengcheng Xi, Won-Sook Lee, and Chang Shu, "*Analysis of segmented human body scans*," Proceedings of Graphics Interface 2007, pp. 19-26, 2007.

[Zhou2010] Shizhe Zhou, Hongbo Fu, Ligang Liu, Daniel Cohen-Or, and Xiaoguang Han, "*Parametric reshaping of human bodies in images*," ACM Transactions on Graphics (TOG), Vol. 29, No. 4, Article No. 126, 2010.